Florida Department of Transportation

Bridge Scour Manual

TABLE OF CONTENTS

LIST OF FIGURES

LIST OF TABLES

LIST OF SYMBOLS

b   pile width (diameter)

b_p prototype pile width

b_{col} column width

b_{pc} pile cap width

d^* dimensionless particle diameter

D^*_{col} effective diameter of the column

D^*_{CS} effective diameter of the complex structure

D^*_{pc} effective diameter of the pile cap

D^*_{pg} effective diameter of the pile group

D_{16} sediment size for which 16 percent of bed material is finer

D_{50} median sediment diameter

D_{84} sediment size for which 84 percent of bed material is finer

D_{90} sediment size for which 90 percent of bed material is finer

f_1 distance between the leading edge of the column and the leading edge of the pile cap

f_2 distance between the side edge of the column and the side edge of the pile cap

F_1 represents the functional dependence of the scour depth at a uniform cross-section pier on the ratio of water depth to pier width (y_0/D^*)

F_2 represents the functional dependence of the scour depth at a uniform cross-section pier on the ratio of depth averaged velocity to sediment critical velocity (V/V_c)

F_3 represents the functional dependence of the scour depth at a uniform cross-section pier on the ratio of pier width to median sediment diameter (D^*/D_{50})

g   acceleration of gravity = 32.17 ft/s^2

H_{col} distance between the bed (adjusted for general scour, aggradation/degradation, and contraction scour) and the bottom of the column

H_{pc} distance between the bed (adjusted for general scour, aggradation/degradation, contraction scour, and column scour) and the bottom of the pile cap

H_{pg} distance between the bed (adjusted for general scour, aggradation/degradation, contraction scour, column scour, and pile cap scour) and the top of the pile group

k   bed roughness height

L_{col} column length

L_{pc} pile cap length

s_m distance between centerlines of adjacent piles in line with the flow in a pile group

s_n	distance between centerlines of adjacent piles perpendicular to the flow in a pile group
sg	ratio of sediment density to the density of water ρ_s / ρ
t	time
t_e	reference time
t_{90}	time to reach 90% of equilibrium scour depth
T	pile cap thickness
T_r	dimensionless parameter in van Rijn's bed form equations
V	mean depth averaged velocity
V_c	critical depth averaged velocity
V_{lp}	depth averaged velocity at the live bed peak scour depth
V_0	depth averaged velocity upstream of the pier
y_s	equilibrium scour depth
y_o	water depth adjusted for general scour, aggradation/degradation, and contraction scour
α	flow skew angle in radians
μ	dynamic viscosity of water
ν	kinematic viscosity of water
ρ	mass density of water
ρ_s	mass density of sediment mineral (example: ρ_s for quartz sand = 165 lb/ft^3)
σ	measure of the sediment gradation = $\sqrt{D_{84} / D_{16}}$
τ	stream bed shear stress
τ_c	critical stream bed shear stress
τ_u	upstream bed shear stress
τ_0	maximum bed shear stress in local scour hole
ϕ	factor for pier shape
$\equiv$	symbol for "equivalent to" (or "defined as")

CHAPTER 1 INTRODUCTION

Bridge scour is the lowering of the streambed at bridge piers and abutments. Bridge scour is the largest cause of bridge failure in the United States and a major factor that contributes to the total construction and maintenance costs of bridges in the United States. Under prediction of design scour depths can result in costly bridge failures and possibly loss of life, while over prediction can result in over design that may significantly affect the construction costs. For these reasons, accurate prediction of scour depths anticipated at a bridge crossing under design flow conditions is essential. Accurate prediction of design scour depths not only depends on adequate prediction methods but on accurate estimates of flow and sediment parameters at the site. Accurate estimates of the design flow and water depth and information on the type and properties of the soil at the site are required. This document provides detailed information on methodologies for estimating local scour and briefly discusses the other categories of scour with references to more detailed information on these topics.

Sediment scour occurs when the amount of sediment removal from an area is greater than the amount entering. Sediment transport is typically divided into two categories: bed load and suspended load. Bed load refers to sediment particles that roll and slide in a thin layer on the stream bed. Sediment particles suspended in the water column by turbulent fluctuations and transported with the flow is referred to as suspended load. Sediment movement is initiated when the forces acting on the particles reaches a threshold value that exceeds the forces keeping them at rest. Water flowing over a sediment bed exert lift and drag forces on the sediment particles. When these forces per unit area (bed shear stress) exceed a critical value (critical shear stress) the sediment bed begins to move. For cohesionless sediments, such as sand, the critical shear stress depends on the mass density and viscosity of the water, the sediment mass density, the size and shape of the sediment particle, the bed roughness, as well as the local water velocity. For cohesive sediments (e.g., muds and clays) and erodible rock, additional water and sediment properties associated with the bonding of the particles also play a role. The local velocity of the water depends on many quantities including the sediment that forms the boundaries of the flow. A change in the sediment boundaries (e.g., deposition or erosion) results in a change in the flow and vice versa. Man-made or natural obstructions to the flow can also change flow patterns and create secondary flows. Any change in the flow can impact sediment transport and thus the scour at a bridge site.

For engineering purposes, sediment scour at bridge sites is normally divided into four categories: 1) lateral migration, 2) aggradation and degradation, 3) contraction scour and 4) local scour. Local scour is further divided into pier and abutment scour. Lateral migration refers to mechanisms that create horizontal changes to the waterway such as river meanders, tidal inlet instability, etc. Aggradation and degradation refer to the vertical raising or lowering of the streambed due to changes taking place up and/or downstream of the bridge (i.e., an overall lowering or rising of the stream bed). Contraction scour results from a reduction in the channel cross-section at the bridge site. This reduction is usually attributed to the encroachment by the bridge abutments and/or the presence of large bridge piers (large relative to the channel cross-section). Abutment scour results from the obstruction to the flow by the bridge abutments and its prediction has been combined with the prediction of contraction scour by some researchers. Local pier scour is likewise the result of a flow obstruction, but one located within the flow field. Fig. 1-1 shows the effect of local scour on a bridge pier. An additional mechanism, bed form propagation through the bridge site, may also play a role. Bed forms refer to the pattern of regular or irregular sediment waves that result from water flow over the sediment bed. These forms may propagate either in the same or in the opposite direction of the flow. Since these undulations in the sediment bed may under certain conditions have large amplitudes, one must also account for their contribution to the lowering of the bed at the bridge site. Additionally, their presence contributes to the overall shape and roughness of the bed, and hence may affect the flow.

The main mechanisms of local scour are: 1) increased mean flow velocities and pressure gradients in the vicinity of the structure; 2) the creation of secondary flows in the form of vortices; and 3) the increased turbulence in the local flow field. Two kinds of vortices may occur: 1) wake and flow separation vortices, downstream of the points of flow separation on the structure; and 2) horizontal axis vortices at the bed and free surface due to stagnation pressure variations along the face of the structure and flow separation at the edge of the scour hole. These phenomena, although relatively easy to observe, are difficult to quantify mathematically.

Local scour is divided into two different scour regimes that depend on the flow and sediment conditions upstream of the structure. Clear-water scour refers to the local scour that takes place under the conditions where sediment is not in motion on a horizontal bed upstream of the structure. If sediment upstream of the structure is in motion, then the local scour is called live-bed scour.

Figure 1-1   Local scour hole at a bridge pier after a flow event.

Most published local scour prediction methodologies/equations, of which there are many, are empirical and, for the most part, based on laboratory-scale data. Historically there has been significant scatter in published laboratory data for a variety of reasons including, tests performed for insufficient durations, inadequate or insufficient instrumentation used, important parameters not being measured, etc. The number of structures, sediment, and flow parameters that influence local scour depths is large and, for practical reasons, must be limited to those with greatest impact when developing a predictive method. This has led to different dimensionless groups of parameters being used, depending on the developer's perception on which parameters are most important. With predictive methods using different parameters, some of which do not adequately represent the physics of the processes involved, and laboratory data that, in some cases is inaccurate, it is not surprising that there can be large differences in their predictions.

Accurate sediment, flow and scour depth measurements are difficult to make for prototype structures. For this reason, field data is typically only used to ensure that predictive methods yield conservative estimates of that observed in the field.

The scour prediction methods presented in this manual have been shown to adequately predict both laboratory and field data that has been screened for accuracy.

3

This manual is organized as follows:

- Chapter 2 discusses total scour at a bridge crossing and presents summaries and references to more detailed treatments of lateral migration, aggradation/degradation and contraction scour.
- Chapter 3 details the calculation of local scour at single, prismatic structures under both clear-water and live-bed scour flow conditions.
- Chapter 4 outlines the procedure for calculation of local scour at bridge piers with more complex geometries including those with buried or partially buried pile caps.
- Chapter 5 discusses additional scour related issues such as scour at multiple structures in close proximity to each other and scour at structures founded in cohesive sediments or erodible rock.

CHAPTER 2 BRIDGE SCOUR

When water flows through a bridge opening with sufficient velocity, the bed, in general, will change in elevation. This change in elevation is more significant near the abutments and piers. The magnitude of these changes depends on many factors including the flow and sediment parameters, structure size and shape, local and global channel characteristics, etc. A net loss of sediment at the site is referred to as sediment scour or simply scour. Knowledge of the maximum scour that will occur during a design flow event or, in the case of bridge piers founded in cohesive sediments, the maximum scour that will occur during the life of the bridge is required for design. Under prediction of these values could result in catastrophic failure and possible loss of life while over prediction can result in over design of the structure, and thus prove costly and economically inefficient. Accurate prediction of scour is, therefore, of the utmost importance. The methods and equations presented in this chapter are the result of years of research on this topic at the University of Florida and more recently at Ocean Engineering Associates, Inc. and INTERA Incorporated.

For analysis purposes, it is convenient to divide bridge scour into the following categories: 1) lateral migration, 2) long term aggradation/degradation, 3) contraction scour, and 4) local structure-induced pier and abutment scour. An additional mechanism, bed form propagation through the bridge site, may also play a role. The combined sum of all five components determines the total scour at a bridge pier or abutment. Even though most of these processes take place simultaneously, for purposes of local scour calculation, the equations presented herein were developed under the assumption that the first three categories plus bed form amplitudes have occurred prior to the start of local and abutment scour. Therefore, general scour, aggradation/degradation, contraction scour and bedform amplitudes must be computed and the bed elevation adjusted prior to calculating local and abutment scour.

2.1. Lateral Migration

For the purposes of this document, lateral migration refers to the bed elevation changes that result from lateral instability of the waterway. This horizontal shifting is divided into two classes. Bridge sites are often classified according to the nature of the flows encountered. Sites that are far removed from the coasts where the flows are not significantly influenced by astronomical tides are referred to as "riverine" sites while those near the coast are called "tidal" sites. The flows at both sites are unsteady, but in general, the time scales are significantly different in the two cases. Additionally, tidal flows often reverse flow direction. In the riverine environment, lateral migration refers to the natural meandering process as illustrated in Fig. 2-1. Meanders in rivers result from transverse oscillation of the thalweg (the deepest part of the channel) within a straight channel. This oscillation initiates formation of self-perpetuating bends in the stream. Although the literature contains relatively little research regarding river meandering, observations indicate characteristics associated with flow in bends. These characteristics include: (1) super-elevation of the water at the outside of the bend, (2) strong downward currents causing potential erosion at the outside of the bend, (3) scour at the outside and deposition of sediment on the inside of the bend that moves the channel thalweg toward the outside of the bend, and (4) a spiral secondary current that directs the bottom current toward the inside of the bend. The overall effect of these mechanisms is to accentuate existing bends in rivers. If a bridge crossing is located near one of these meanders, the horizontal migration of the stream can result in an overall raising or lowering of the bed. Therefore, this process is treated as a component of sediment scour. For more information on this topic the reader is referred to the NCHRP Web-only Document 67 "Methodology for Predicting Channel Migration" (National Academies of Sciences, 2004) and Federal Highway Administration's (FHWA) Hydraulic Engineering Circular Number 20 (HEC-20) (Lagasse, et al., 2012).

In coastal waters, tidal inlet instability is similar in that the channel migrates laterally to affect a change in bed elevation at piers located in the vicinity of the inlet. Unimproved inlets (inlets without jetties) are, in general, much less stable and are prone to larger and more frequent lateral shifts. Inlet stability depends on several variables including the magnitude and variability of longshore sediment transport, incident waves, the tidal prism, other inlets in the system, coastal structures in the vicinity, etc. Fig. 2-2 through Fig. 2-4 contain aerials that illustrate channel migration at Ft. George Inlet in Jacksonville, Fl from 1992 to 2021. The channel cross section at

the bridge has seen significant change over the 29-year period as can be seen in the photographs. For more information on inlet instability the reader is referred to Dean and Dalrymple (2002).

Figure 2-1   Aerial view of the lower Mississippi River.

Figure 2-2   Ft. George Inlet 1992.
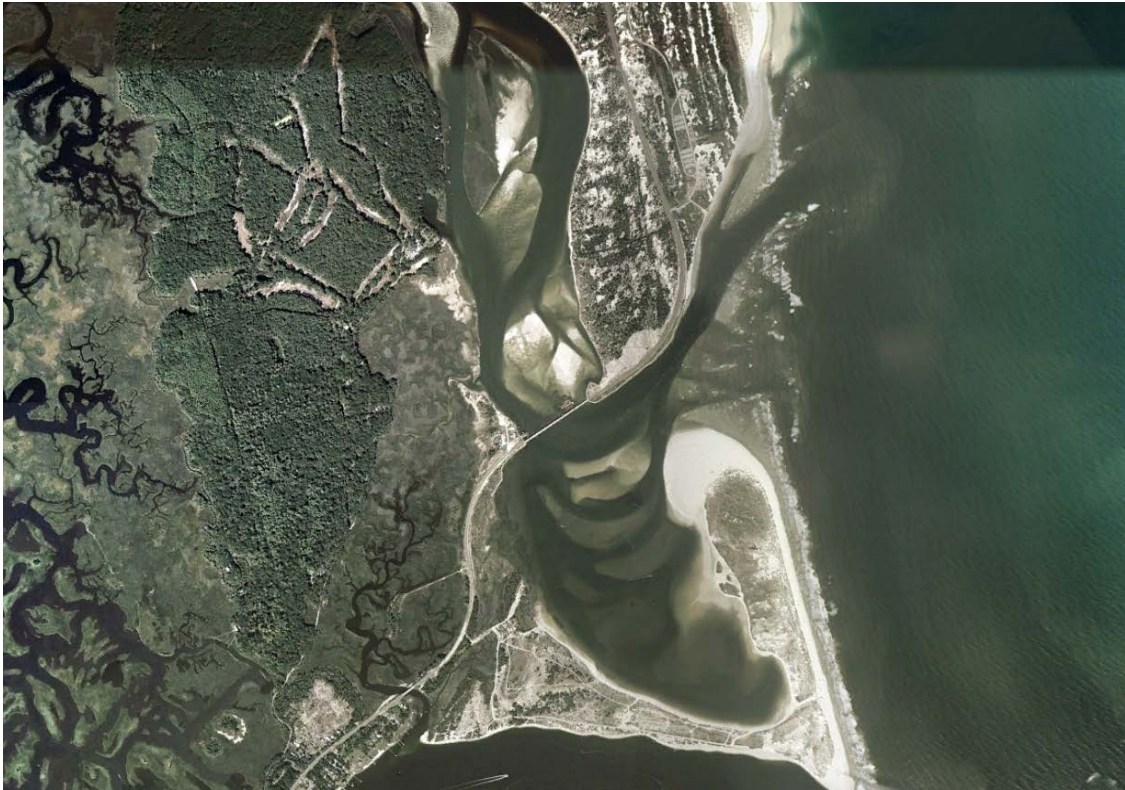
Figure 2-3   Ft. George Inlet 2003 (source: Google Earth).
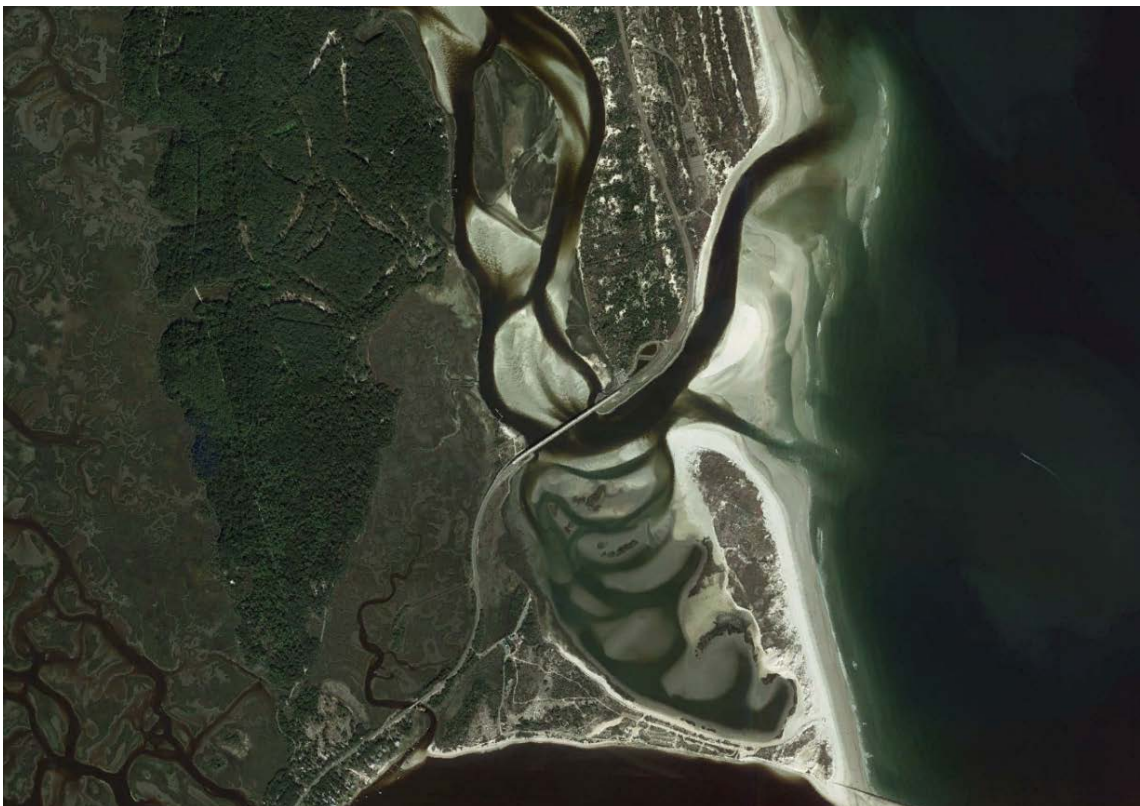
Figure 2-4   Ft. George Inlet 2021 (source: Google Earth).

2.2. Long Term Aggradation and Degradation

Whereas general scour refers to bed elevation changes that result from lateral instability, aggradation and degradation is associated with the overall vertical stability of the bed. Long term aggradation and degradation refers to the change in the bed elevation over time over the entire reach of the water body. For riverine conditions, manmade or natural changes in the system may produce erosion or deposition with time over the entire reach of the water body. Anything that changes the sediment supply of a river reach can impact the bed elevation at the bridge site. Examples of these changes include the erection or removal of an upstream dam, changes in upland drainage basin characteristics (e.g., land use changes), upstream mining in the channel, etc. For information on aggradation/degradation in riverine environments, the reader is referred to the FHWA's Hydraulic Engineering Circular Number 18 (Arneson, et al., 2012) and its references.

Similar processes exist in tidal waters. However, in general, prediction of these processes is more difficult due to the complex geometry of the flow boundaries, reversing flows, wave climate, etc. As with riverine locations, historical information about the site and the quantities that impact the sediment movement in the area are very useful in estimating future changes in bed elevation at the site. For more information refer to the US Army Corps of Engineers' Coastal Engineering Manual (2002).

2.3. Contraction Scour

Contraction scour occurs when a channel's cross-section is reduced by natural or manmade features. Possible constrictions include the construction of long causeways to reduce bridge lengths (and costs), the placement of large (relative to the channel cross-section) piers in the channel, abutment encroachment, and the presence of headlands (see Fig. 2-5 and Fig. 2-6). The reduction of cross-sectional area results in an increase in flow velocity. This may result in more sediment leaving than entering the area and thus an overall lowering of the bed in the contracted area. This process is known as contraction scour.

For design flow conditions that have long durations, such as those created by stormwater runoff in rivers and streams in relatively flat country, contraction scour can reach near equilibrium depths. Equilibrium conditions exist when the sediment leaving and entering a section of a stream are equal. Laursen's contraction scour prediction equations were developed for these

conditions. A summary of Laursen's equations is presented below. For more information and discussion, the reader is referred to HEC-18 (2012).
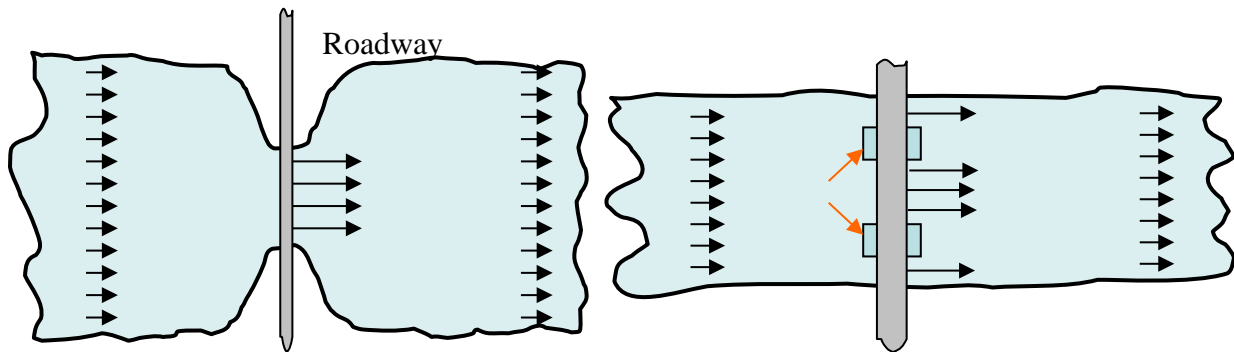
Figure 2-5   Two manmade features that create a contracted section in a channel.

Figure 2-6   An example of manmade causeway islands that create a channel contraction.

2.3.1. Steady, uniform flows

For steady, uniform flow situations one-dimensional hydraulic models are usually adequate for

estimating design flow velocities. If, in addition, the design flow event is of long duration, such as a riverine runoff event in relatively flat terrain, equilibrium contraction scour equations can estimate design contraction scour depths. Laursen's contraction scour equations [Laursen (1960)] were developed for these situations. However, predictions using these equations tend to be conservative, even for long duration flows, since the rate of erosion decreases significantly with increased scour depth. That is, unless the design flow duration is extremely long, equilibrium depths are not achieved. Laursen developed different equations for clear-water and live-bed scour flow regimes. Both equations are designed for situations with relatively simple flow boundaries. A brief summary of the equations is presented herein. The reader is referred to HEC-18 (2012) for more information.

2.3.1.1. Live bed contraction scour equation

The live-bed scour equation assumes that the upstream flow velocities are greater than the sediment critical velocity, V_c. For these conditions the equation is:

$$y_s = y_2 - y_o = \text{average contraction scour}$$

2.1

where

$$\frac{y_2}{y_1} = \left(\frac{Q_2}{Q_1}\right)^{\frac{6}{7}} \left(\frac{W_1}{W_2}\right)^{K_1},$$

2.2

$y_1 =$ Average depth in the upstream channel, ft (m),
$y_2 =$ Average depth in the contracted section after scour, ft (m),
$y_0 =$ Average depth in the contracted section <u>before scour</u>, ft (m)
$Q_1 =$ Discharge in the upstream channel transporting sediment, ft^3/s (m^3/s),
$Q_2 =$ Discharge in the contracted channel, ft^3/s (m^3/s),
$W_1 =$ Bottom width of the main upstream channel that is transporting bed material, ft (m),
$W_2 =$ Bottom width of the main channel in the contracted section less pier widths, ft (m)
$K_1 =$ Exponent listed in Table 2-1below (dimensionless).

Table 2-1   Determination of exponent, K_1

$\dfrac{V_*}{\omega}$	K_1	Mode of Bed Material Transport
<0.50	0.59	Mostly contact bed material discharge
0.50 to 2.0	0.64	Some suspended bed material discharge
>2.0	0.69	Mostly suspended bed material discharge

where

V_* = $(\tau_o/\rho)^{0.5}$, shear velocity in the upstream section, ft/s (m/s),

ω = Fall velocity of bed material based on the D_{50}, ft/s (m/s) (Fig. 2-7),

g = Acceleration of gravity, 32.17 ft/s^2 (9.81 m/s^2),

τ_o = Shear stress on the bed, lb$_f$/ft^2 [Pa (N/m^2)], and

ρ = Density of water, slugs/ft^3 (kg/m^3).
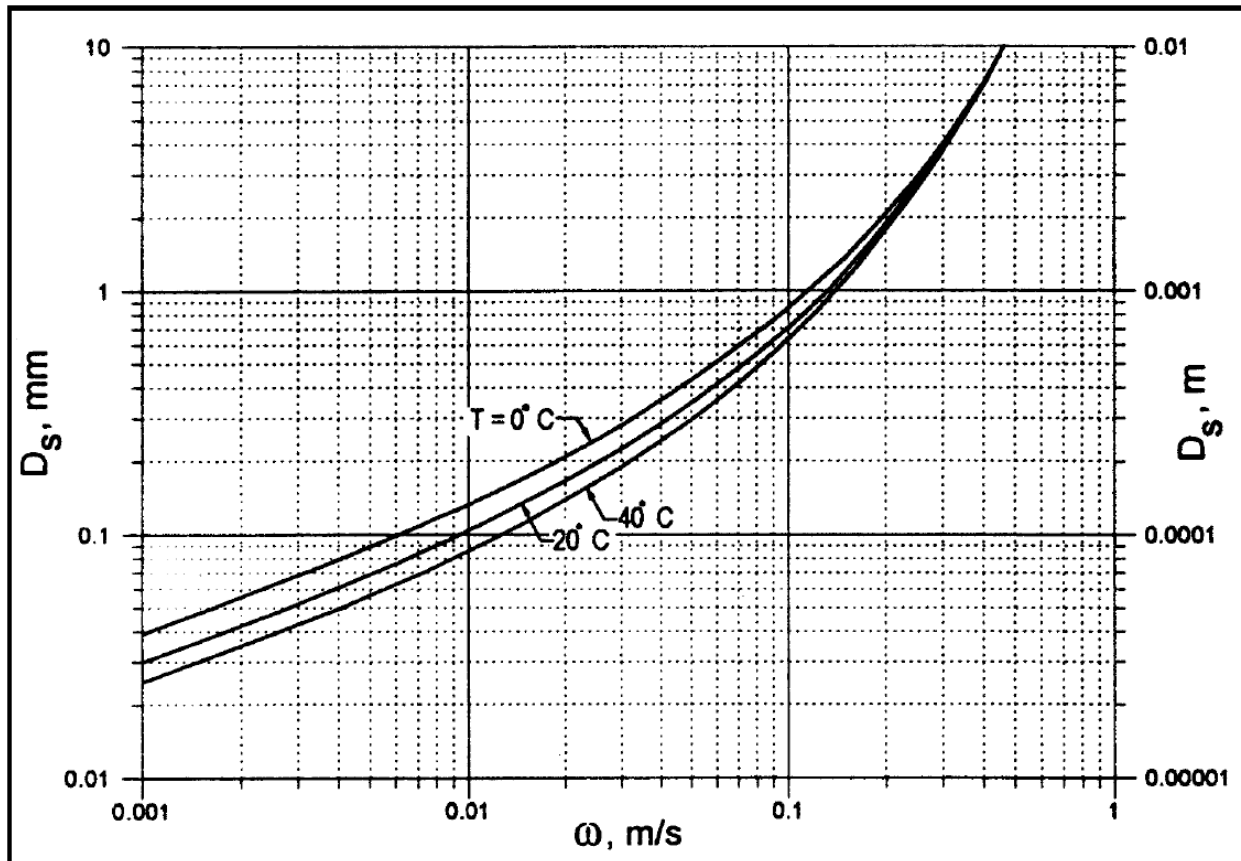
Figure 2-7   Fall velocity of sediment particles having specific gravity of 2.65 [taken from HEC-18, (2012)]. D_s is the sediment diameter.

2.3.1.2.   Clear-water contraction scour equation

The clear-water scour equation assumes that the upstream flow velocities are less than the sediment critical velocity. The equation is:

12

$$y_s = y_2 - y_o = \text{average contraction scour} \qquad 2.3$$

where

y_2 = Average equilibrium contraction scour, ft (m)

$$y_2 = \left[\frac{K_u Q^2}{D_m^{\frac{2}{3}} W^2} \right]^{\frac{3}{7}} \qquad 2.4$$

Q = Discharge through the bridge or on the set-back overbank area at the bridge associated with the width W, ft^3/s (m^3/s),

D_m = Diameter of the smallest non-transportable particle in the bed material (1.25 D_{50}) in the contracted section, ft (m),

D_{50} = Median diameter of bed material, ft (m),

W = Bottom width of the contracted section less pier widths, ft (m),

y_o = Average existing depth in the contracted section, ft (m), and

K_u = 0.0077 (when using English units).

For a more detailed discussion of these equations, the reader is referred to the HEC-18 (2012).

2.3.2. Unsteady, complex flows

There are many situations where Laursen's contraction scour equations are not appropriate including cases where: 1) the flow boundaries are complex, 2) the flows are unsteady (and/or reversing), and 3) the duration of the design flow event is short, etc. These situations are better analyzed using two-dimensional, flow and sediment transport models for estimating contraction scour depths (e.g., USACE's CMS Flow or DHI's MIKE-21). Just what constitutes a short or long duration flow event is not well defined, but is dependent on several factors including site conditions, type of design flow, as well as the type of sediment. As such, one must rely on engineering judgment and experience when making these determinations.

2.4. Bed Forms

When cohesionless sediments are subjected to currents and/or surface waves, bed forms can occur. These bed features are divided into several categories (ripples, mega ripples, dunes, sand waves, antidunes, etc.) according to their size, shape, method of generation, etc. Since some of these wave-like features can have large amplitudes, they must be accounted for in the

determination of design scour depths. This is particularly true for structures with buried pile caps that may be uncovered by these bedforms. There are a number of predictive equations in the literature for estimating bed form height and length [e.g. Tsubaki-Shinohara (1959), Ranga Raju-Soni (1976), Allen (1968), Fredsoe (1980), van Rijn (1993)]. One of these formulations is presented below.

The following methods and equations for estimating bed form heights and lengths were developed by Leo C. van Rijn. The details of this work and the work of other researchers can be found in van Rijn (1993).

The first step in van Rijn's procedure establishes the type of bed form that will exist for the flow and sediment conditions of interest. This is accomplished by computing the values of the dimensionless parameters T_r and d^* and then referring to Table 2-2. The equations in Table 2-3 estimate the bed form height and length given the bed form type.

Table 2-2   Bed classification for determining bed forms.

Transport Regime		Particle Size	
		$1 \leq d_* \leq 10$	$d_* > 10$
Lower	$0 \leq T_r \leq 3$	Mini-Ripples	Dunes
	$3 \leq T_r \leq 10$	Mega-Ripples and Dunes	Dunes
	$10 \leq T_r \leq 15$	Dunes	Dunes
Transition	$15 \leq T_r \leq 25$	Washed-Out Dunes, Sand Waves	
Upper	$T_r \geq 25,\ Fr < 0.8$	(Symmetrical) Sand Waves	
	$T_r \geq 25,\ Fr > 0.8$	Plane Bed and/or Anti-Dunes	

The expressions for T_r, d_* and Fr are as follows:

$$T_r = \frac{\tau' - \tau_c}{\tau_c}$$

2.5

where the critical bed shear stress, τ_c, can be estimated using Eq. ?? in chapter 3.

$$\tau' \equiv \rho g \left(\frac{V}{C'} \right)^2 ,$$

$$C' \equiv 32.6 \frac{ft^{1/2}}{s} \log_{10}\left(\frac{12y_0}{3D_{90}}\right) = 18 \frac{m^{1/2}}{s} \log_{10}\left(\frac{12y_0}{3D_{90}}\right),$$

$$d_* \equiv D_{50}\left[\frac{(sg-1)g}{v^2}\right]^{1/3},$$

$sg \equiv \dfrac{\rho_s}{\rho} =$ mass density of sediment divided by mass density of water,

$v \equiv \dfrac{\mu}{\rho}$ = kinematic viscosity of water,

$g \equiv$ acceleration of gravity $= 32.17\ ft/s^2$,

$y_0 \equiv$ water depth just upstream of structure,

$D_{90} \equiv$ grain diameter of which 90% of sediment has a smaller value, and

$Fr \equiv$ Froude Number $= \dfrac{V}{\sqrt{gy_0}}$.

Table 2-3   Bed form length and height (van Rijn, 1993).

Bed Form Classification	Bed Form Height (Δ)	Bed Form Length (λ)
Mega- Ripples[1]	$0.02y_0\left[1-\exp(-0.1T_r)\right]\ (10 - T_r)$	$0.5y_0$
Dunes	$0.11y_0\left(\dfrac{D_{50}}{y_0}\right)^{0.3}\left[1 - \exp(-0.5T_r)\right](25 - T_r)$	$7.3y_0$
Sand Waves	$0.15y_0(1 - Fr^2)\left\{1 - \exp\left[-0.5(T_r - 15)\right]\right\}$	$10y_0$

$$\frac{\tau}{(\rho_s - \rho) g D_{50}}$$

Reynolds Number Based on Friction Velocity $= \dfrac{\sqrt{\dfrac{\tau}{\rho}}\, D_{50}}{\nu}$
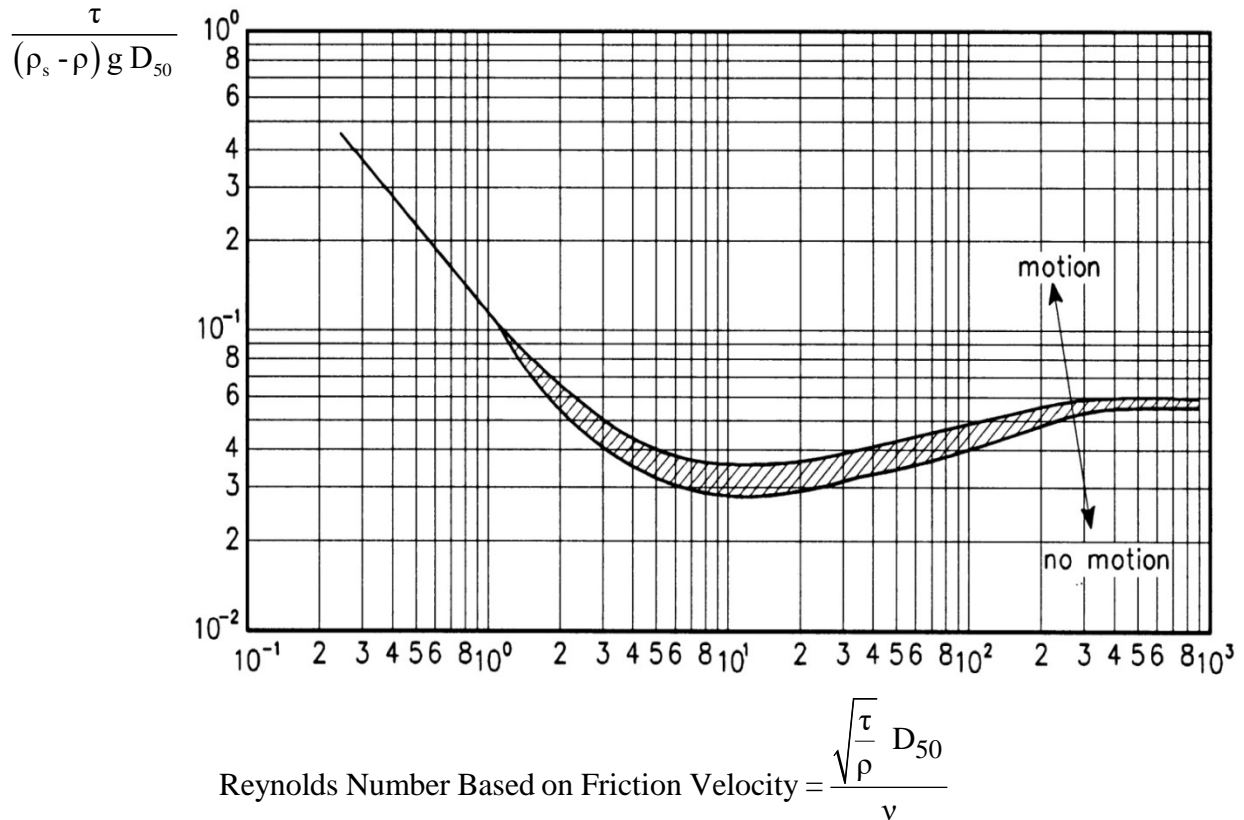
Fig. 2-8   Critical bed shear stress as a function of sediment particle diameter, Shields (1936).

2.5. Local Scour

When water flows around a structure located in or near an erodible sediment bed, the increased forces on the sediment particles near the structure may remove sediment from the vicinity of the structure. This erosion of sediment is referred to as structure-induced sediment scour (local scour or pier scour). For cohesionless sediments, the scour hole usually takes the form of an inverted cone with a slope approximately equal to the angle of repose for the sediment in water. The deepest depth of the scour hole is of greatest interest to the geotechnical/structural engineer in the design of a new (or in the stability analysis of an existing) structure. Therefore, scour hole depth, or more simply scour depth, refers to the maximum depth within the scour hole. For a given steady flow velocity and water depth, the scour depth increases with time until it reaches a maximum value known as the equilibrium scour depth, y_s. The integrity of the structure supported by the sediment is often highly dependent on the depth of the scour hole. Much of the early scour research was for scour at single circular piles. As a result, methods and equations for estimating scour at more complex structures often employ of and build on this knowledge. Chapter 3 is devoted to methods for computing equilibrium scour depths at singular uniform

16

cross-section structures (piles). Chapter 4 presents methods and equations for more complex bridge pier structures.

CHAPTER 3 LOCAL SCOUR AT PIERS WITH UNIFORM CROSS-SECTIONS

3.1. Introduction

There are many local scour depth prediction equations in the literature as well as review papers that compare the various equations and methodologies. Most of these equations are empirical and based primarily on small scale laboratory data. While many of these equations yield reasonable results for laboratory scale structures and sediments, they can differ significantly in their prediction of scour depths at large, prototype scale structures. This chapter discusses the formulation of equilibrium local scour depth prediction equations for single, uniform cross-section structures. These equations were originally developed by Professor D. Max Sheppard and his graduate students at the University of Florida but have evolved over the years with contributions from Professor Bruce Melville at the University of Auckland. They are referred to as the Sheppard/Melville (or simply as the S/M) equations and are included in the more recent versions of the FHWA's Hydraulic Engineering Circular Number 18 (HEC-18). For more information about this methodology, as well as its comparison with other predictive methods can be found in National Academies of Sciences (2011).

This section discusses the flow field near a cylindrical pile in a steady flow, as described by various researchers. The flow field in the immediate vicinity of a structure is quite complex, even for simple structures such as circular piles. One of the dominant features of the local flow field is the formation of secondary flows in the form of vortices. Many investigators (e.g., Shen et al., 1966, Melville, 1975) believe that these vortices are the most important mechanisms of local scour (at least during certain phases of the scour evolution).

Vortices, with near horizontal axes are formed at the bed and near the water surface on the upstream edge of the structure. These are referred to as the "horseshoe" and "surface" vortices, respectively. The term "horseshoe" is derived from the shape that the vortex takes as it wraps around the pile and trails downstream when viewed from above (Fig. 3.1). Shen et al. (1966) describes the horseshoe vortex system in detail. The horseshoe vortex is initiated by the stagnation pressure gradient on the leading edge of the structure resulting from the bottom boundary layer of the approaching flow. That is, the variation in flow velocity from zero at the bed to the value at the surface causes a variation in stagnation pressure on the leading edge of the structure. The largest stagnation pressure

occurs at the elevation of the highest velocity. In its simplest form, the horseshoe vortex system is composed of two vortices, a large one next to the structure and one adjacent small counter rotating vortex. For more complex flows and structure shapes, multiple unsteady vortices are formed which periodically shed and are swept downstream. Clearly, the geometry of the structure is important in determining the strength of the vortex system. Blunt nosed structures create the most energetic vortex systems.
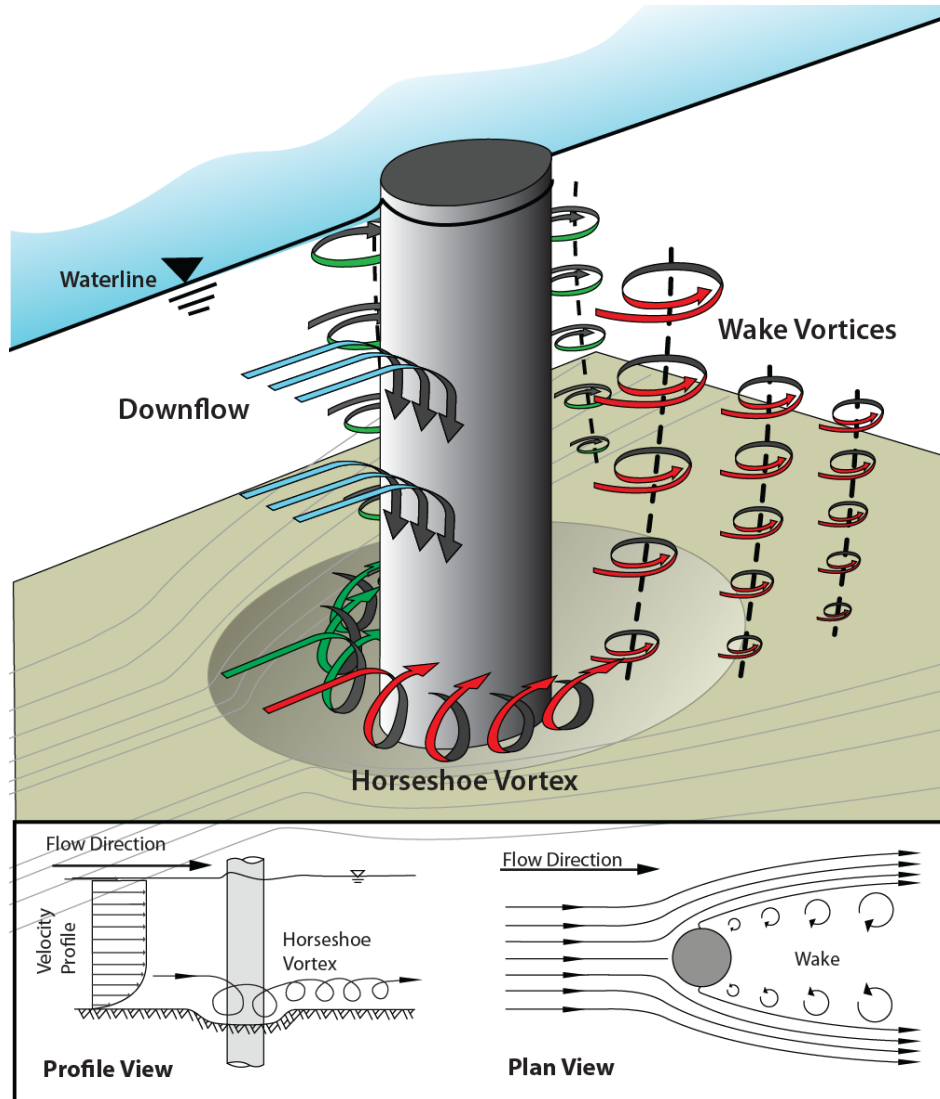

Figure 3-1   Schematic drawing of local scour processes at a cylindrical pier.

Melville (1975) measured mean flow directions, mean flow magnitude, turbulent flow fluctuations, and computed turbulent power spectra around a circular pile for flatbed, intermediate and

19

equilibrium scour holes. He found that a strong vertical downward flow developed ahead of the cylinder as the scour hole enlarged. The size and circulation of the horseshoe vortex increased rapidly and the velocity near the bottom of the hole decreased as the scour hole was enlarged. As the scour hole develops further, the intensity of the vortex decreases and reaches a constant value at the equilibrium stage.

Although the horseshoe vortex is considered the most important scouring mechanism for steady flows, the wake vortex system is also important. Wake vortices are created by flow separation on the structure. Large scour holes may also develop downstream from piers under certain circumstances (e.g., Shen et al., 1966). With their vertical component of flow, wake vortices act somewhat like a tornado. They put the bed material in suspension, where it is carried downstream by the mean flow.

More recently another potential scour mechanism was identified [Sheppard (2004)]. This mechanism results from the pressure gradient field generated by the presence of the structure in the flow. The pressure field near the bed is, for the most part, determined by the pressure field in the main body of flow. Potential flow theory shows that there are significant variations in pressure in the flow field near the structure. These pressure gradients impose pressure forces on the sediment grains that can be much larger than the drag forces due to the flow around the grains. The pressure gradients reduce in magnitude with increasing structure size; therefore, they are more important for laboratory scale than for prototype scale structures. The results of the analysis presented in Sheppard (2004) help explain the dependence of equilibrium scour depth on the various dimensionless groups discussed in the next section.

3.2. Equilibrium Scour Depths in Steady Flows

There is usually a distinction made between local scour that occurs at flow velocities less than and greater than the sediment critical velocity (the velocity required to initiate sediment movement on a horizontal bed just upstream of the structure). If the velocity is less than the sediment critical velocity, the scour is known as "clear-water scour". If the velocity is greater than the sediment critical velocity, the scour is called "live-bed scour". The following discussion is limited to sediments that are cohesionless, such as sand. For sediments such as silts, muds, clays, and rock, additional parameters must be considered to account for the forces that bond the particles together.

For most structures in a steady flow, the local scour depth varies in magnitude around the structure. In this discussion the term <u>local scour depth</u> (or just <u>local scour</u>) refers to the depth of the deepest point in the local scour hole.

Equilibrium local scour depth depends on a number of fluid, sediment and structure parameters. Eq. 3.1 expresses this mathematically as

$$y_s \equiv f\left(\rho, \mu, g, D_{50}, \sigma, \rho_s, y_0, V, D^*, \Theta\right),$$

3.1

where

y_s ≡ the equilibrium scour depth (maximum local scour depth after the flow duration is such that the depth is no longer changing),

f ≡ symbol meaning "function of ",

ρ and ρ_s ≡ density of water and sediment respectively,

μ ≡ dynamic viscosity of water (depends primarily on temperature),

g ≡ acceleration of gravity,

D_{50} ≡ median diameter of the sediment,

σ ≡ gradation of sediment,

y_0 ≡ depth of flow upstream of the structure,

V ≡ depth average velocity upstream of the structure,

D^* ≡ effective diameter of structure, i.e. the diameter of circular pile that would experience the same scour depth as the structure for the same sediment and flow conditions. For a circular pile D^* is simply the diameter of the pile.

Θ ≡ parameter quantifying the concentration of fine sediments in suspension .

The most important dimensionless groups for local scour can be obtained from the quantities given in Eq. 3.1. These eleven quantities can be expressed in terms of three fundamental dimensions: force, length and time. According to the Buckingham π theorem, eight (11 variables, 3 fundamental dimensions) independent dimensionless groups exist for this situation. An example of these eight groups is given in Eq. 3.2

$$\frac{y_s}{D^*} = f\left(\frac{y_0}{D^*}, \frac{V}{\sqrt{g\,y_0}}, \frac{\rho_s}{\rho}, \frac{VD^*\rho}{\mu}, \frac{V}{V_c}, \frac{D_{50}}{D^*}, \sigma, \Theta\right)$$

<div align="right">3.2</div>

where V_c is the critical depth-averaged velocity (the velocity required to initiate sediment motion on a flat bed).

The large number of variables (and, therefore, dimensionless groups) affecting local scour processes has resulted in researchers presenting their data in a wide variety of ways. This has made it difficult to compare results from different investigations and to some extent has slowed progress in local scour research. As with any complex problem, some of the groups are more important than others. It is impractical (if not impossible) to include all of the groups in an analysis of the problem. The question becomes "which of the groups are the most important for local scour processes?"

Based on the importance of Froude Number ($V/\sqrt{gy_0}$) in open channel flows, some of the earlier researchers chose to employ this group to account for flow intensity and water depth. For example, the equation referred to as the CSU (Colorado State University) equation, which is presented in the current version of the FHWA HEC-18 (2012), includes the Froude Number. A wide variety of groups and combinations of groups have been proposed over the years, each working reasonably well for at least the range of (mostly laboratory) data used in their development. Some researchers (including the authors of this manual) have found that the parameters in Eq. 3.3 can describe equilibrium scour depths for a wide range of conditions.

$$\frac{y_s}{D^*} = f\left(\frac{y_0}{D^*}, \frac{V}{V_c}, \frac{D^*}{D_{50}}, \sigma, \Theta\right)$$

<div align="right">3.3</div>

If the sediment is near uniform in size $(\sigma \leq 1.5)$ the effect of σ is small and can be neglected. If the size distribution is large, the equilibrium scour depth can be significantly reduced due to natural armoring as the finer grains are removed leaving only the larger grains which require more energy for their removal.

The suspended fine sediment in the water column (often referred to as washload) has been shown to reduce equilibrium scour depths in laboratory tests. However, more research is needed before the level of scour reduction can be quantified. The effects of σ is discussed further in Chapter 5.

The discussion thus far in this chapter has been limited to single, circular piles. This can be

extended to other prismatic structures such as the three common shapes as shown in Table 3-1. Note that circular and square shapes are just special cases where the lengths are equal to the widths.

The shape of the structure and its projection onto a vertical plane normal to the flow determine the effective diameter of the structure, D*. The shape and projection coefficients for three common shapes are presented in Tables 3-1 and 3-2. Situations where the structure is not both stream bed and water surface penetrating are covered in Chapter 4.

$$D^* \equiv K_s K_p \qquad\qquad 3.4$$

Table 3-1   Shape factor for common pier shapes.

Structure Shape (Plan View)	Shape Coefficient, K_s
General Constraints: $0 \leq \alpha \leq \dfrac{\pi}{2}$ and structure must be both water surface and bed penetrating If $L/b > 2$ set $L/b = 2$	
	$K_s = 0.8(1 - L/b)(\alpha/\pi)^2 + 0.8(L/b - 1)(\alpha/\pi) + 1$
	$K_s = (9.6 - 4.8(L/b))(\alpha/\pi)^2 - (4.8 - 2.4(L/b))(\alpha/\pi) + 1.2$
	$K_s = \begin{cases} \text{for } 0 \leq \alpha \leq \pi/4 \quad 1 \leq L/b \leq 2 \\ -4.8(\alpha/\pi)^2 + 2.4(\alpha/\pi) + 0.9 \\ \text{for } \pi/4 < \alpha \leq \pi/2 \quad 1 \leq L/b \leq 2 \\ 1.2L/b - 2.4)(\alpha/\pi) + 1.8 - 0.3L/b \end{cases}$
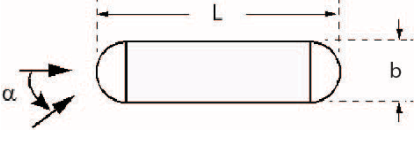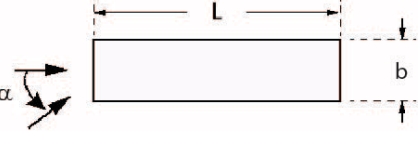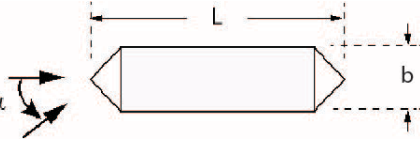
Table 3-2   Projection factor for common pier shapes

Structure Shape (Plan View)	Projection Coefficient, K_p
	$K_p = b + (L-b)\sin(\alpha)$ $0 \le \alpha \le \pi/2$
	$K_p = b\cos(\alpha) + L\sin(\alpha)$ $0 \le \alpha \le \pi/2$
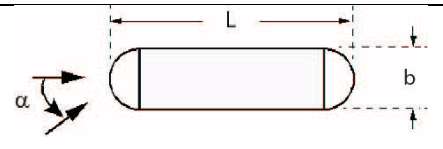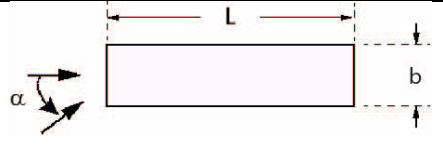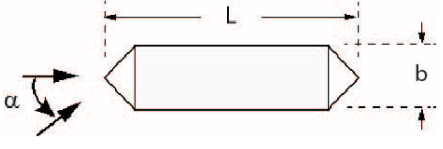
The following equilibrium local scour depth equations were developed by Sheppard and his graduate students at the University of Florida and improved during the research by Sheppard, Melville and Demir (National Academies of Science 2011). They are empirical and based primarily on laboratory data obtained by Sheppard in four different Laboratories (University of Florida in Gainesville, Florida, Colorado State University in Fort Collins, Colorado, University of Auckland in Auckland, New Zealand and the Conte USGS-BRD Laboratory in Turners Falls, Massachusetts).

In the clear-water scour range ($0.4 \le \dfrac{V}{V_c} \le 1.0$)

$$\frac{y_s}{D^*} = 2.5 F_1 F_2 F_3 \tag{3.5}$$

In the live-bed scour range below the live-bed peak velocity ($1.0 < \dfrac{V}{V_c} \le \dfrac{V_{lp}}{V_c}$)

$$\frac{y_s}{D^*} = F_1 \left[2.2 \left(\frac{\frac{V}{V_c}-1}{\frac{V_{lp}}{V_c}-1} \right) + 2.5 F_3 \left(\frac{\frac{V_{lp}}{V_c} - \frac{V}{V_c}}{\frac{V_{lp}}{V_c}-1} \right) \right], \tag{3.6}$$

and in the live-bed scour range above the live bed peak velocity ($\dfrac{V}{V_c} > \dfrac{V_{lp}}{V_c}$)

24

$$\frac{y_s}{D^*} = 2.2 F_1, \tag{3.7}$$

where

$$F_1 \equiv \tanh\left[\left(\frac{y_0}{D^*}\right)^{0.4}\right] \tag{3.8}$$

$$F_2 \equiv \left\{1 - 1.2\left[\ln\left(\frac{V}{V_c}\right)\right]^2\right\} \tag{3.9}$$

$$F_3 \equiv \left[\frac{\left(\dfrac{D^*}{D_{50}}\right)}{0.4\left(\dfrac{D^*}{D_{50}}\right)^{1.2} + 10.6\left(\dfrac{D^*}{D_{50}}\right)^{-0.13}}\right] \tag{3.10}$$

$$
\begin{aligned}
V_1 &= 5V_c, \\
V_2 &= 0.6\sqrt{g\,y_0}, \text{ and} \\
V_{1p} &= \text{live bed peak velocity} = \begin{cases} V_1 \text{ for } V_1 > V_2 \\ V_2 \text{ for } V_2 > V_1 \end{cases}.
\end{aligned} \tag{3.11}
$$

$$
V_c = \begin{cases}
\dfrac{0.066}{1 - 500 D_{50}} \log_{10}\left(3 y_o / D_{50}\right) & 0.10\text{mm} \leq D_{50} \leq 0.60\text{mm} \\[2ex]
\dfrac{-0.041}{1 + 0.44 \log_{10}\left(D_{50}\right)} \log_{10}\left(5 y_o / D_{50}\right) & 0.60\text{mm} < D_{50} \leq 1.14\text{mm} \\[2ex]
\left(-0.085 + 6.7 D_{50}^{\,0.5}\right) \log_{10}\left(4.4 y_o / D_{50}\right) & 1.14\text{mm} < D_{50} \leq 5.70\text{mm} \\[2ex]
5.62 D_{50}^{\,0.5} \log_{10}\left(4 y_o / D_{50}\right) & 5.70\text{mm} < D_{50}
\end{cases} \tag{3.12}
$$

Note that Equation 3.12 is dimensional and both y_0 and D_{50} should be in meters. The variations of normalized equilibrium scour depth, y_s/D^*, with the three dimensionless groups, y_0/D^*, V/V_c, and D^*/D_{50} are shown graphically in Fig. 3-2 through Fig. 3-4.
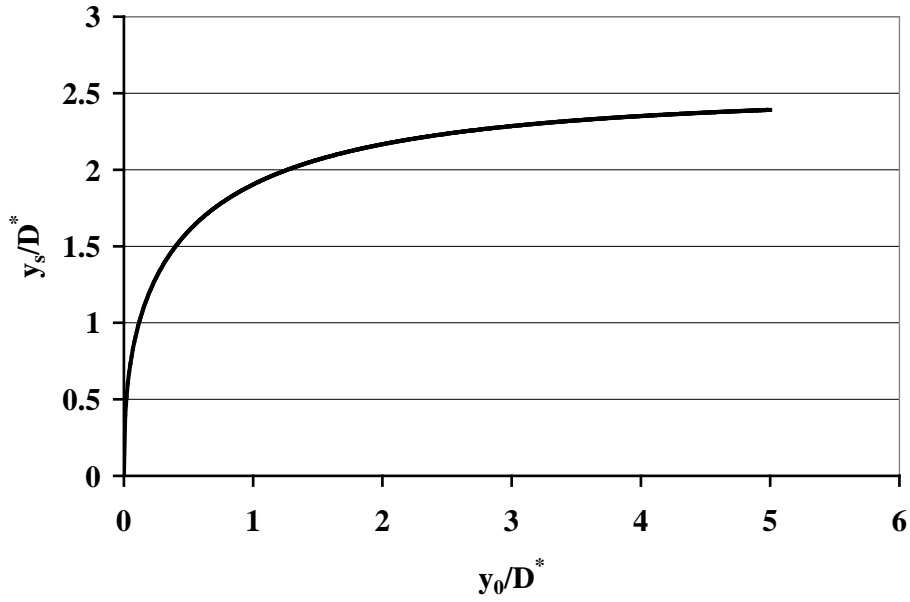
Figure 3-1 Equilibrium scour depth dependence on y_0/D^* ($V/V_c = 1$ and $D^*/D_{50} = 46$).
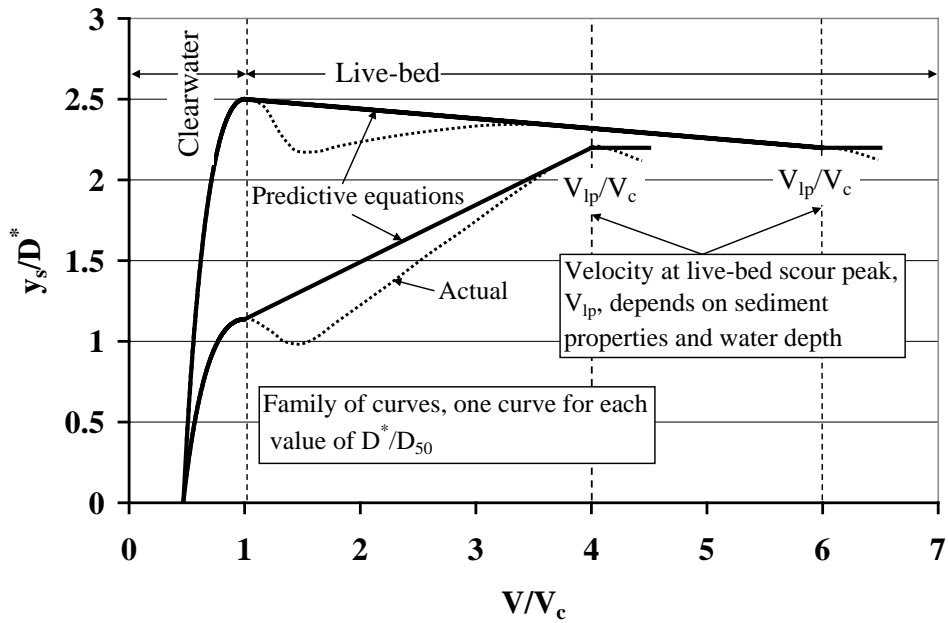
Figure 3-2 Equilibrium scour depth dependence with flow intensity, V/V_c (for $y_0/D^* > 3$ and constant values of D^*/D_{50}).
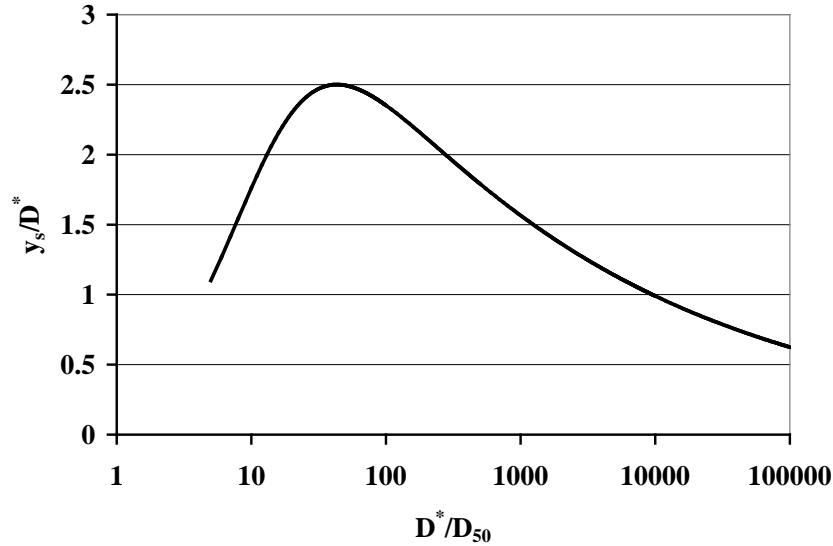
Figure 3-3 Equilibrium scour depth dependence on D^*/D_{50} for $y_0/D^* > 3$ and $V/V_c=1$.

Fig. 3-2 shows the dependence of scour depth on the aspect ratio, y_0/D^* while holding V/V_c and D^*/D_{50} constant. Fig. 3-3 shows the variation of scour depth with flow intensity, V/V_c for constant y_0/D^* and D^*/D_{50}. Fig. 3-4 shows the dependence of scour depth on D^*/D_{50} for constant y_0/D^* and V/V_c. The data indicates that there are two local maximums in the scour depth versus V/V_c plots. The first local maximum occurs at transition from clear-water to live-bed scour conditions, i.e., at $V/V_c =1$. The second maximum, referred to here as the "live-bed peak" is thought to occur at the flow conditions where the bed forms disappear (i.e., the bed planes out). The velocity that produces the live-bed scour peak is called the live-bed peak velocity and is denoted by V_{lp}.

Data obtained by the authors and other researchers clearly show that the equilibrium scour depth decreases with increasing velocity just beyond the transition peak before proceeding to the live-bed peak. Since Eqs. 3.4 - 3.11 are intended for design applications, no attempt was made to include this reduction in scour depth in the predictive equations. For slowly varying flows, the structure will experience the transition peak en route to the live-bed design flow condition.

In the clear-water scour range, equilibrium scour depth is very sensitive to changes in the flow intensity, V/V_c. To a lesser extent, scour depth is also sensitive to the magnitude of the live-bed peak velocity, V_{lp}. It is therefore important to employ the same methods applied during the development of the equations when computing V_c and V_{lp}. The sediment critical velocity, V_c, is calculated using Eq. 3.13.

CHAPTER 4 SCOUR AT PIERS WITH COMPLEX GEOMETRIES

4.1. Introduction

Most large bridge piers are complex in shape and consist of several clearly definable components. While these shapes are sensible and cost effective from a structural standpoint, they can present a challenge for those responsible for estimating design sediment scour depths at these structures. This chapter presents a methodology for estimating scour depths at a class of structures composed of up to three components.

<u>Methodology for Estimating Local Scour Depths at Complex Piers</u>

This section presents a methodology for estimating equilibrium local scour depths at bridge piers with complex pier geometries, located in cohesionless sediment and subjected to steady flow conditions. These methods apply to structures composed of up to three components as shown in Fig. 4.1. In this document, these components are referred to as the: 1) column, 2) pile cap, and 3) pile group. The equations presented in this section were developed by D. Max Sheppard with assistance from Huseyin Demir. They are empirical and based on a substantial number of laboratory tests. They are intended to be applied as described in this chapter for piers that are similar in shape to the generic structure for which they were derived.

Most published data and information on local scour are for single circular piles. Likewise, the most accurate predictive equations for equilibrium scour depth are for single circular piles. It seems reasonable then that predictive methods for local scour at more complex structures would build upon and take advantage of this knowledge and understanding. The methods presented in this chapter are based on the assumption that a complex pier can be represented (for the purposes of scour depth estimation) by a single circular (water surface penetrating) pile with an "effective diameter" denoted by D^*. The magnitude of D^* is such that the scour depth at a circular pile with this diameter is the same as the scour depth at the complex pier for the same sediment and flow conditions. The problem of computing equilibrium scour depth at the complex pier is therefore reduced to one of determining the value of D^* for that pier and applying the single pile equations presented in Chapter 3 to this pile for the sediment and flow conditions of interest.

28
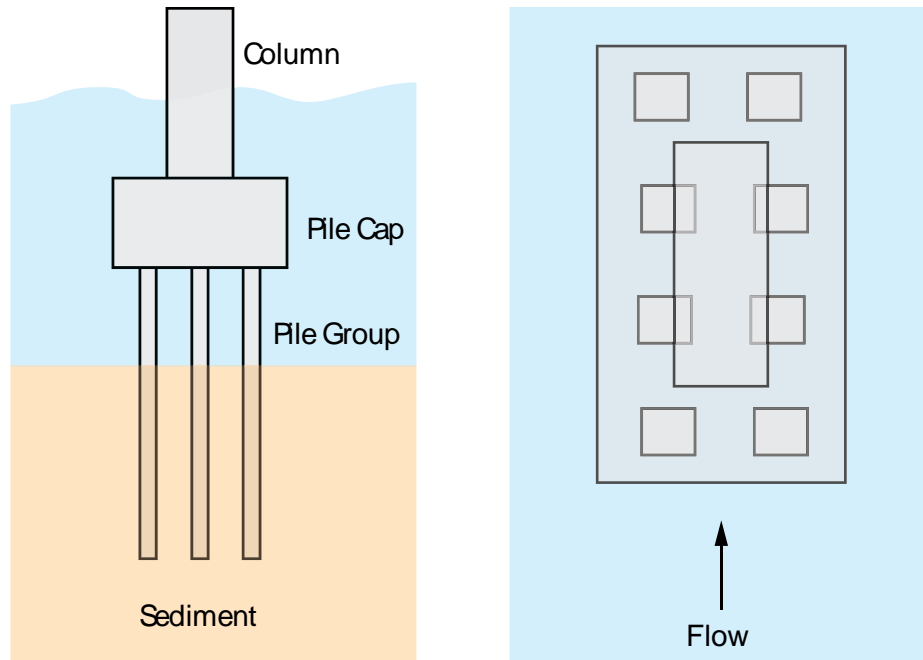
Figure 4-1   Complex pier configuration considered in this document. The pile cap can be located above the water, in the water column or below the bed.

The methodology is based on several assumptions. First, the structure can be divided into up to three components as shown in Figure 4-2. Next, for scour computation purposes, each component can be replaced by a single, surface penetrating, circular pile with an effective diameter (D*) that depends on the shape, size and location of the component and its orientation relative to the flow as shown in Figure 4-3. For components that are initially buried their effective diameter will also depend on how much sediment is removed by components located above the bed. Finally, the addition of structure component effective diameters to obtain the effective diameter of the complete structure implies linearity (i.e. a component's presence does not impact the effective diameter of the other components) which is obviously not the case. However, if the major interactions are recognized and accounted for then acceptable estimations of equilibrium scour depth predictions can be achieved. The equations are designed to applicable in any logical combination of the components (e.g., the combination of a column and pile group without a pile cap is disallowed) and for all practical ranges of their positions. Since the equations are empirical and cover a relatively wide range of conditions, they may not provide consistent results when pushed to the extreme, e.g. evaluating a column as a water surface penetrating pile group with one pile in the pile group.
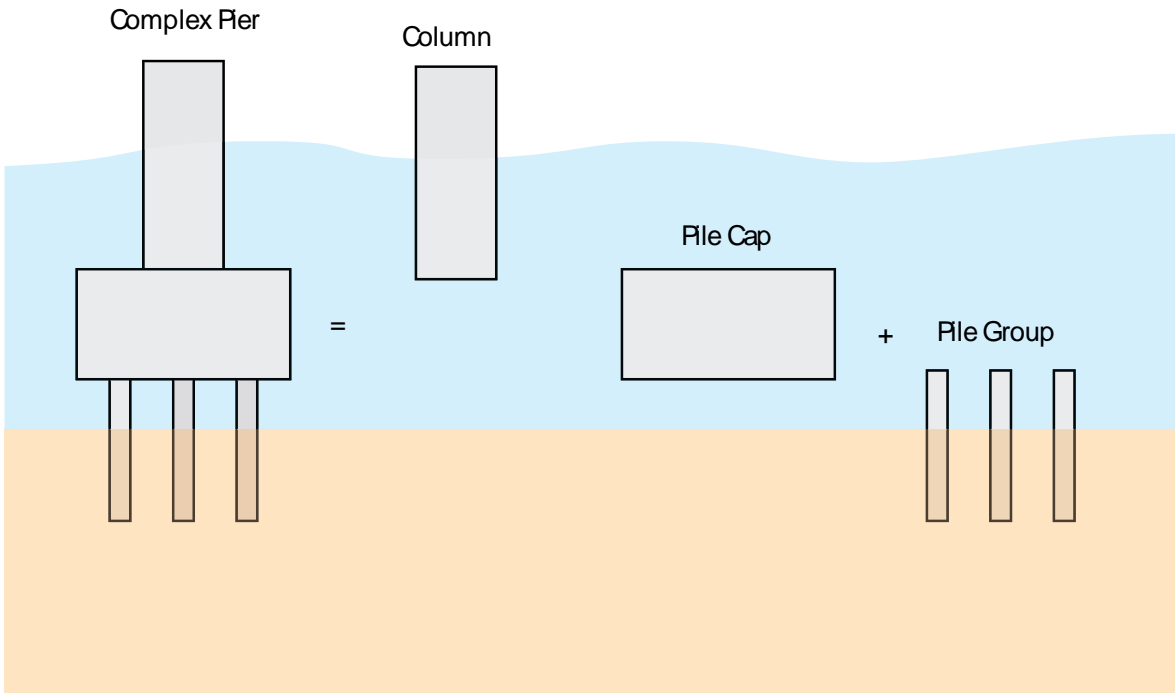
Figure 4-2   Schematic drawing of a complex pier showing the 3 components: column, pile cap and pile group.

This methodology is for estimating local, structure-induced scour only. Lateral channel migration, aggradation/degradation, contraction scour, and bed form heights must be established prior to applying this procedure. The information needed to compute local scour depths at complex piers is summarized below:

1.   Lateral migration, aggradation/degradation, contraction scour, and bed form heights;

2.   External dimensions of all components making up the pier including their vertical positions relative to the pre-local scoured bed;

3.   Median sediment grain diameter; and

4.   Water depth and depth-averaged flow velocity just upstream of the structure for the flow condition of interest.

Figure 4-3   Effective diameter for complex pier components.
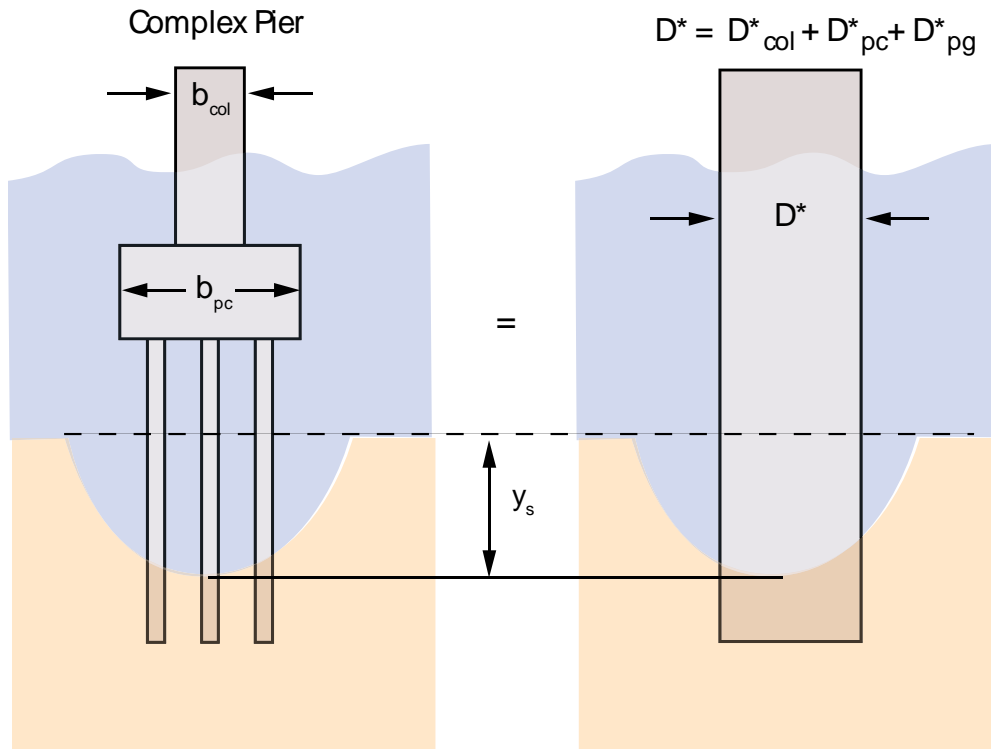
Figure 4-4   Effective diameter for a complex pier.

Laboratory data provides the following insight into the dependence of the effective diameter of the components of the complex structure considered here on the various parameters involved.

Column

The effective diameter of a column primarily depends on:

1. Width
2. Length
3. Length/width ratio
4. Flow skew angle
5. Shape
6. Location in the water column
7. Interaction between the column and pile cap

Shape consideration is like that of the prismatic structure but is influenced by the presence of the pile cap if one exists. The effective diameter increases as the base of the column progresses from the water surface to a depth beyond that of the scour hole.

<u>Pile Cap</u>

The effective diameter of the pile cap primarily depends on:

1. Width
2. Length
3. Length/width ratio
4. Flow skew angle
5. Shape
6. Thickness
7. Location in the water column

As with the column the width, length and flow skew angle all contribute to the pile cap's effective diameter. The pile cap thickness and location are also important. In general, it increases in effective diameter size from when its base enters the water surface until it is partially submerged in the stream bed. When the upper surface of the pile cap is at or below the bottom of the scour hole its effective diameter is reduced to zero.

<u>Pile Group</u>

The effective diameter of the pile group depends on:

1. Individual pile width, shape
2. Number of piles normal to the (non-skewed) flow
3. Number of piles in-line with the (non-skewed) flow
4. Spacing of the piles
5. Pile group skewness to the flow
6. Location of the top of the piles in the water column

Estimation of the effective diameter of the pile group involves several parameters, some of which are like those for the column and pile cap. The additional parameters that must be considered are the number of piles normal to and in-line with the non-skewed flow as well as their spacing.

<u>Methodology for Estimating the Effective Diameter of Complex Pier Components</u>

The approach presented herein begins with establishing a vertical datum below the stream bed that is lower than the maximum scour depth at the structure for the sediment and flow conditions under consideration. All vertical measurements are then referenced to this datum. Simple algebraic equations (linear, quadratic, etc.) can then express the dependence of the structure component's effective diameter on the various independent parameters. Best fit methods were used with

laboratory data to evaluate coefficients in the equations. The equations were then tested against a much larger data set. The test data set included a range of structure, sediment and flow conditions.

<u>Vertical Datum</u>

The location of the vertical datum is determined by computing a conservative estimate of the maximum scour depth that would occur at the structure under the sediment and flow conditions of interest. This involves making conservative estimates of the effective diameters of the components of the structure. Substituting the sum of these diameters along with the sediment and flow parameters of interest into Eqs. 3.4-3.11 yields a somewhat overly conservative estimate of the maximum scour depth at the structure for the specified conditions. This process exposes the components (and parts of components) that are likely to be subjected to water flow during the scour event. A vertical datum is then located at the bottom of the computed scour hole. This conservative local scour depth estimate is then refined with more accurate subsequent calculations to provide the final local scour estimate. Section 4.3 presents the calculation of this vertical datum.

4.2. Complex Pier Local Scour Calculation

The total D* for the structure can be approximated by the sum of the effective diameters of the components making up the structure i.e.,

$$D_{CS}^* \equiv SF(D_{col}^* + D_{pc}^* + D_{pg}^*)$$ 4.1

where

$SF \equiv$ design safety factor, 1.25,
$D_{CS}^* \equiv$ effective diameter of the complex structure,
$D_{col}^* \equiv$ effective diameter of the column,
$D_{pc}^* \equiv$ effective diameter of the pile cap,
$D_{pg}^* \equiv$ effective diameter of the pile group,

The local scour for the complex pier, $y_{s(complex\ structure)}$ is calculated using D_{CS}^* with. Eqs. 3.4 through 3.11. A final correction is made after this calculation as explained in Section 4.7. The methodology for calculating each component and the vertical datum is detailed in the following sections. The methodology is valid for skew angles between 0 and $\pi/4$. If the skew angle is more than $\pi/4$, the structure should be rotated 90 degrees so that the skew angle is less than $\pi/4$. Pointed structures

that are rotated are treated as rectangular structures.

A definition sketch showing the parameters employed in the equations is shown in Figure 4-1. Note that the units of the flow skew angle, α, is radians.
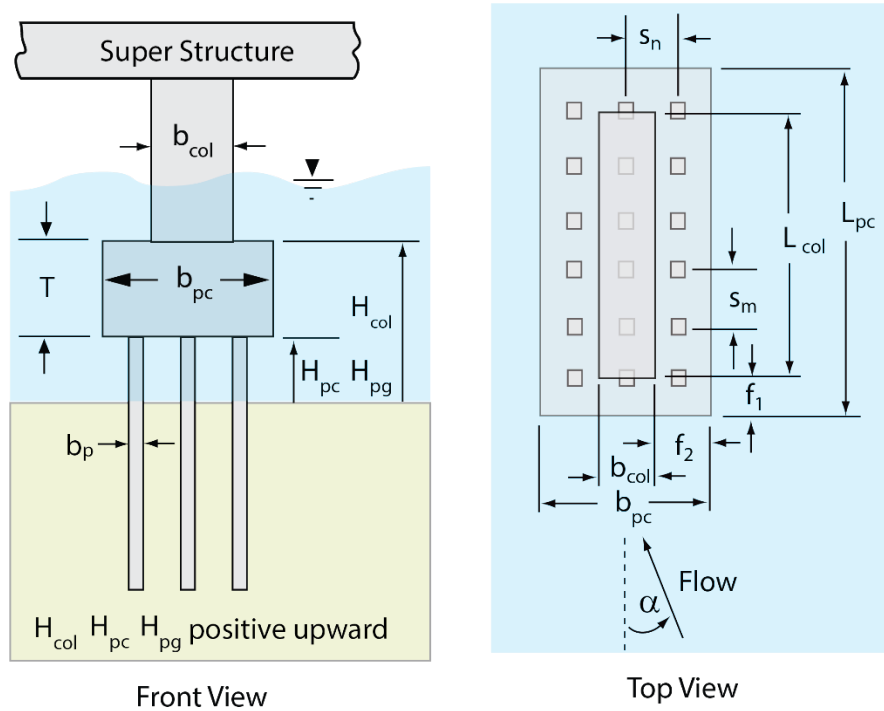
Figure 4-5   Complex pier sketch showing dimensions employed in the equations.

4.3. Vertical Datum

The projection of the width of a structural component onto a vertical plane that is normal to the flow is required in the computation of the effective diameter. The water depth impacts the equilibrium local scour depth at the structure for depths up to about 4 to 8 times the effective diameter of the structure. The water depth is an integral part of the scour depth predictive equations and therefore for structures located in deeper water, limits must be placed on the depth used in the equations. An initial water depth limit is made and refined later in the analyses.

Effective diameters can be calculated from Eqs. 4.2-4.4

$$
\begin{aligned}
K_{colp} &\equiv \text{column projection factor} \\
&= b_{col}\cos(\alpha) + L_{col}\sin(\alpha)
\end{aligned}
\qquad 4.2
$$

K_{pcp} ≡ pile cap projection factor

$$= b_{pc} \cos(\alpha) + L_{pc} \sin(\alpha)$$

4.3

K_{pgpi} ≡ initial pile group projection factor

$$= b_p \left(n\cos(\alpha) + m\sin(\alpha) \right)$$

4.4

The initial limitation on the water depth is made with Eqs. 4.5

$$y_{0maxi} = 8\max\left(K_{colp}, K_{pcp}, K_{pgpi} \right)$$

$$y_0 = \begin{cases} y_0 & 0 \le y_0 \le y_{0maxi} \\ y_{0maxi} & y_0 > y_{0maxi} \end{cases}$$

4.5

Initial estimates of the effective diameters of the column, pile cap and pile group are computed using the following equations.

4.3.1. Column Effective Diameter (for locating vertical datum)

D_{coli}^{*} ≡ Initial column effective diameter estimate

$$= 1.8 K_{cols} K_{colp} K_{colhi}$$

4.6

The shape factors for the column and pile cap are computed at this point and employed for both initial and final calculations, similar to projection factors that have been previously calculated. They are dependent on the structure shape, length to width ratio, and flow skew angle.

4.3.1.1. Column Shape factor

$LOB_{col} = L_{col}/b_{col}$

If $LOB_{col} < 1$ set $LOB_{col} = 1/LOB_{col}$ and $(\alpha/\pi) = (0.5 - \alpha/\pi)$

If $LOB_{col} > 2$ set $LOB_{col} = 2$

4.7

Shape factor for a Round Nose structure:

$$K_{cols} = 0.8(1 - LOB_{col})(\alpha/\pi)^2 + 0.8(LOB_{col} - 1)(\alpha/\pi) + 1$$

4.8

Shape factor for a Square Nose structure:

$$K_{cols} = (9.6 - 4.8 LOB_{col})(\alpha/\pi)^2 - (4.8 - 2.4 LOB_{col})(\alpha/\pi) + 1.2$$

4.9

Shape factor for a Pointed Nose structure:

$$K_{cols} = -4.8(\alpha/\pi)^2 + 2.4(\alpha/\pi) + 0.9 \qquad \qquad 4.10$$

4.3.1.2. Initial Column Vertical Location Factor

$K_{colhi} \equiv$ initial column vertical position factor

$$= \begin{cases} 0 & H_{col} > y_0 \\ 1 - H_{col}/y_0 & 0 \le H_{col} \le y_0 \\ 1 & H_{col} < 0 \end{cases} \qquad \qquad 4.11$$

4.3.2. Pile Cap Effective Diameter (for locating vertical datum)

$$D_{pci}^* = 1.8 \, K_{pcs} K_{pcp} K_{pchi} K_{Ti} \qquad \qquad 4.12$$

K_{pcs}= Pile Cap Shape Factor, same equation as column, but using pile cap parameters

K_{pchi}= Pile Cap Vertical Location Factor, same equation as column, but using pile cap parameters

$$K_{Ti} = \text{accounts for the pile cap thickness} = (T/y_0) \quad \text{if } K_{Ti} > 1, \text{ set} = 1 \qquad \qquad 4.13$$

4.3.3. Pile Group Effective Diameter (for locating vertical datum)

$D_{pgi}^* \equiv$ initial pile group effective diameter estimate

$$= 3.5 \, K_{pgs} K_{pgpi} K_{pghi} \qquad \qquad 4.14$$

$K_{pgs} \equiv$ Pile group shape factor

$\qquad = 1.4$

4.3.3.1. Pile Group Vertical Location Factor

$K_{pghi} \equiv$ Initial pile group vertical position factor

$$= \begin{cases} 1 & H_{pg} > y_0 \\ (H_{pg} + 3K_{pgpi})/(y_0 + 3K_{pgpi}) & y_0 \ge H_{pg} > -K_{pgpi} \\ 0 & H_{pg} < -K_{pgpi} \end{cases} \qquad \qquad 4.15$$

4.3.4. Vertical Datum Application

The conservative estimate for the complex structure to establish the location of the vertical datum is the sum of the initial effective diameters of the structure components.

$D_{csi}^{*} \equiv$ initial estimate of the effective diameter of the complex structure

$\qquad = D_{coli}^{*} + D_{pci}^{*} + D_{pgi}^{*}$

4.16

Prior to computing the conservative scour depth that will be used to locate the vertical datum, an improved maximum water depth is computed.

$Y \equiv$ improved upper limit on water depth (measured from stream bed)
to be used in the following calculations:

4.17

$$= \begin{cases} y_0 & y_0 \leq 8D_{csi}^{*} \\ 8D_{csi}^{*} & y_0 > 8D_{csi}^{*} \end{cases}$$

Having a conservative estimate for the structure effective diameter an estimate of the maximum local scour depth, $y_{s(max)}$, is computed from this diameter and the sediment and the flow conditions in Eqs. 3.4-3.11.

The vertical datum is located a distance $y_{s(max)}$ below the stream bed as shown in Figure 4-5.
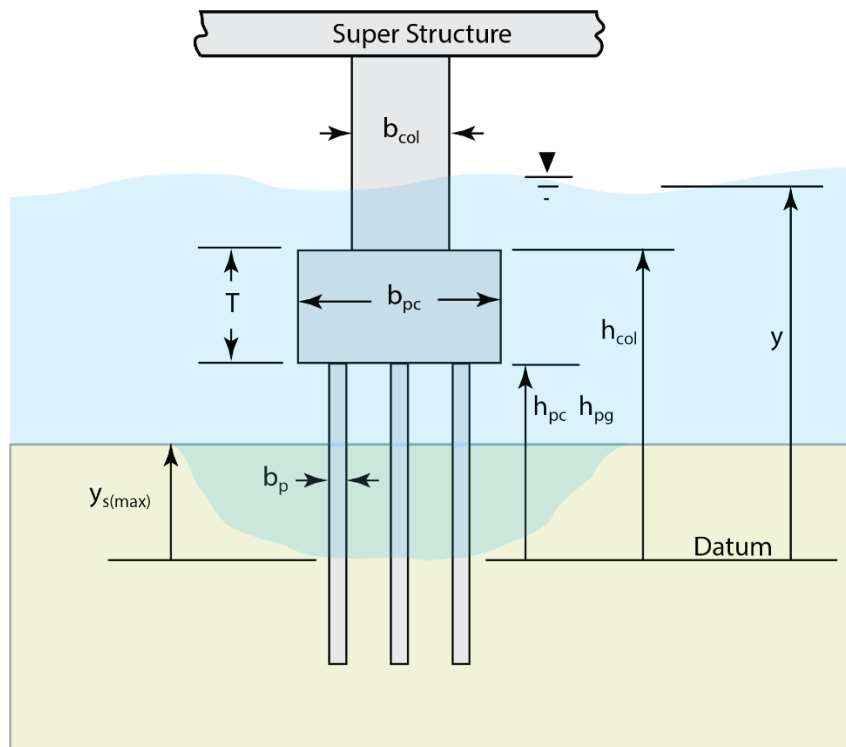
Figure 4-6   Complex structure definition sketch showing location of the vertical datum.

All vertical dimensions are referenced to the vertical datum for the final scour depth calculations as

shown in Figure 4-5.

$$y = Y + y_{s(max)}$$
$$h_{col} = H_{col} + y_{s(max)}$$
$$h_{pc} = H_{pc} + y_{s(max)}$$
$$h_{pg} = H_{pg} + y_{s(max)}$$

4.18

4.4. Column Effective Diameter

The effective diameter of the column without the impact of the pile cap, $D^*_{col\_alone}$ is computed first:

$$D^*_{col\_alone} \equiv K_{cols}K_{colp}K_{LOBcol}$$

4.19

The scour depth produced by the column alone, y_{scol_alone}, (without the effect of the pile cap) for the flow and sediment conditions of interest is computed by substituting $D^*_{col\_alone}$ into Eqs. 3.4 – 3.11. If the scour produced by the column alone does not reach the top of the pile cap, then the scour at the complex pier is that produced by the column alone y_{scol_alone}.

That is, if $(y_{smax} - y_{scol\_alone}) \geq (h_{pc} + T)$, then

$$D^*_{CS} \equiv \text{ effective diameter of the complex pier}$$
$$= D^*_{col\_alone} \text{ and}$$
$$y_{s(complex\ structure)} = y_{scol\_alone}$$

4.20

When this is the case, there is no need to compute the effective diameters of the pile cap and pile group or the pile cap effect on the column. Otherwise continue with the following computations.

$$D^*_{col} \equiv K_{cols}K_{colp}K_{colh}K_{LOB}K_{colf}$$

The shape factors are the same as computed in the initial calculations. The projection factors are provided in Table 3-2. The factors for vertical location, effects of structure length to width ratio and impact of the pile cap on the effective diameter of the column are computed as follows.

4.4.1. Vertical Position Factor

The sketch in Figure 4-6 shows the approximate dependence of the column effective diameter on

the position of the bottom of the column.

$$K_{colh} = \begin{cases} 0 & h_{col} > y \\ 0.65\left[(y - h_{col})/(y - y_{s(max)})\right]^3 & y_{s(max)} \leq h_{col} \leq y \\ 1 - 0.35\left(h_{col}/y_{s(max)}\right)^2 & 0 \leq h_{col} \leq y_{s(max)} \\ 1 & h_{col} < 0 \end{cases} \qquad 4.21$$
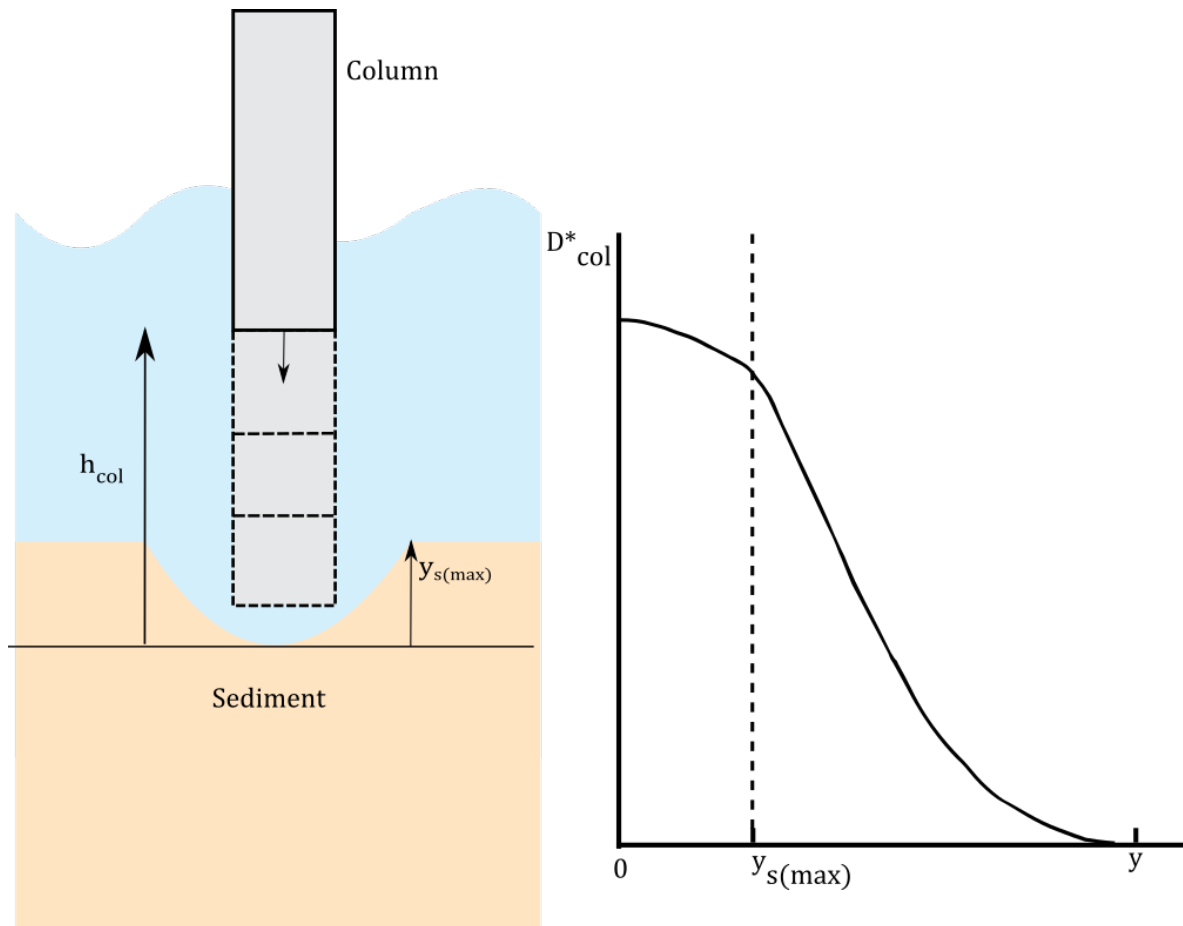
Figure 4-7   Sketch showing how the effective diameter changes with the location of the bottom of the column.

4.4.2. Column Length to Width Factor

The effective width and length of the column are computed using Eqs. 4.22 (see Fig. 4.7).

40

$$b_{col\_e} = b_{col}\cos(\alpha) + L_{col}\sin(\alpha)$$

$$L_{col\_e} = L_{col}\cos(\alpha) + b_{col}\sin(\alpha) \qquad\qquad 4.22$$

$$LOB_{col\_e} = L_{col\_e} / b_{col\_e}$$

$$f_{lob\_col} = \begin{cases} 0.5(LOB_{col\_e})^3 - 0.75(LOB_{col\_e})^2 + 1.25 & LOB_{col\_e} \le 1 \\ 1 & LOB_{col\_e} > 1 \end{cases} \qquad 4.23$$
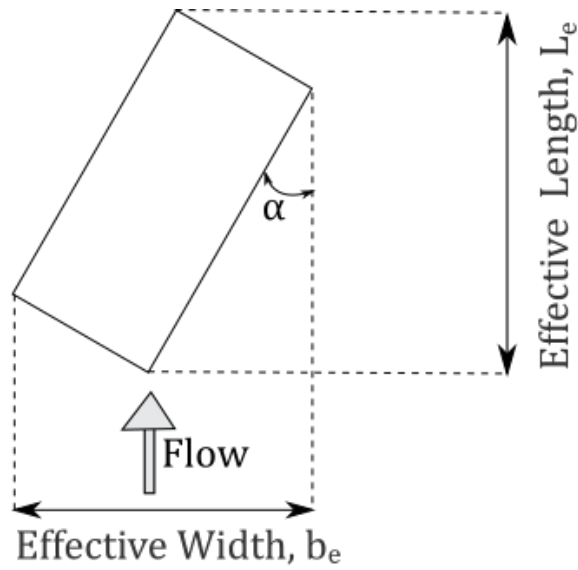
Figure 4-8   Sketch showing effective length and width which are the same for all three shapes.

$$y_{mm} = y_{s(max)} + 0.2y \qquad\qquad 4.24$$

$$
f_{hcol} = \begin{cases} \dfrac{1}{f_{lob\_col}} & h_{col} > y_{mm} \\[4mm] 1 + \left(\dfrac{\left(1 - f_{lob\_col}\right)}{f_{lob\_col}} \right)\left(\dfrac{h_{col} - y_{s(max)}}{y_{mm} - y_{s(max)}} \right) & y_{s(max)} \le h_{col} \le y_{mm} \\[4mm] 1 & h_{col} < y_{s(max)} \end{cases}
\qquad 4.25
$$

$$
K_{LOBcol} = \left(f_{lob\_col} \right)\left(f_{hcol} \right) \qquad\qquad 4.26
$$

4.4.3. Pile Cap Effect on Column Factor

When a pile cap exists, and it is larger than the column this reduces the effective diameter of the column. The amount of the reduction is estimated using the following equations.

The front and side overhangs (difference between lengths and widths of pile cap and column) are:

$$
\begin{aligned}
f_1 &= (L_{pc} - L_{col})/2 \\
f_2 &= (b_{pc} - b_{col})/2
\end{aligned}
\qquad\qquad 4.27
$$

A combination of the overhangs is used in the analysis favoring the leading-edge overhang (that in the direction of the flow).

$$
f = (2/\pi)(f_2 - f_1)\alpha + f_1 \qquad 0 \le \alpha \le \pi/2 \qquad\qquad 4.28
$$

The ratio of overhang to projected column width is:

$$
f_{ratio} = f / K_{colp} \qquad\qquad 4.29
$$

The impact of this ratio on the effective diameter of the column depends on the location of the junction of the column and pile cap in the water column (i.e. h_{col}). The ratio value that reduces the effective diameter of the column to zero is estimated by the following expression:

$$
ff = \begin{cases} 0.3 & h_{col} > y \\ 1.3\left[(y - h_{col})/(y - y_{s(max)})\right]^2 + 0.3 & y \ge h_{col} \ge y_{s(max)} \\ 1.6 & y_{s(max)} > h_{col} \end{cases}
\qquad 4.30
$$

The multiplicative factor that accounts for the impact of the pile cap on the effective diameter of the

42

column is then:

$$K_{colf} = \begin{cases} 1-(f_{ratio}/ff) & 0 \leq f_{ratio} \leq ff \\ 0 & f_{ratio} > ff \end{cases} \qquad 4.31$$

4.5. Pile Cap Effective Diameter

As with the column, the pile cap effective diameter is a function of its shape, projection, vertical location in the water column and its length to width ratio,

$$D_{pc}^{*} \equiv K_{pcs}K_{pcp}K_{pch}K_{LOBpc} \qquad 4.32$$

The shape factors are the same as computed in the initial calculations. The projection factors are provided in Table 3-2.

4.5.1. Vertical Position Factor

Figures 4-8 and 4-9 illustrate the procedure for estimating the pile cap vertical position factor.
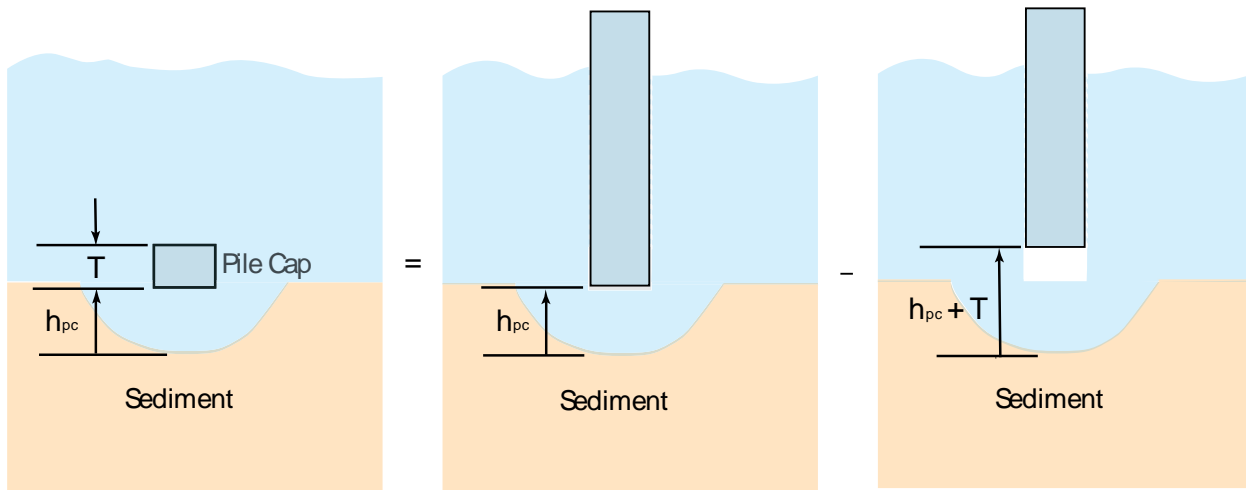
Vertical Position Factor for Pile Cap

Figure 4-9   Sketch indicating how the pile cap vertical location factor, K_{pch}, is computed.
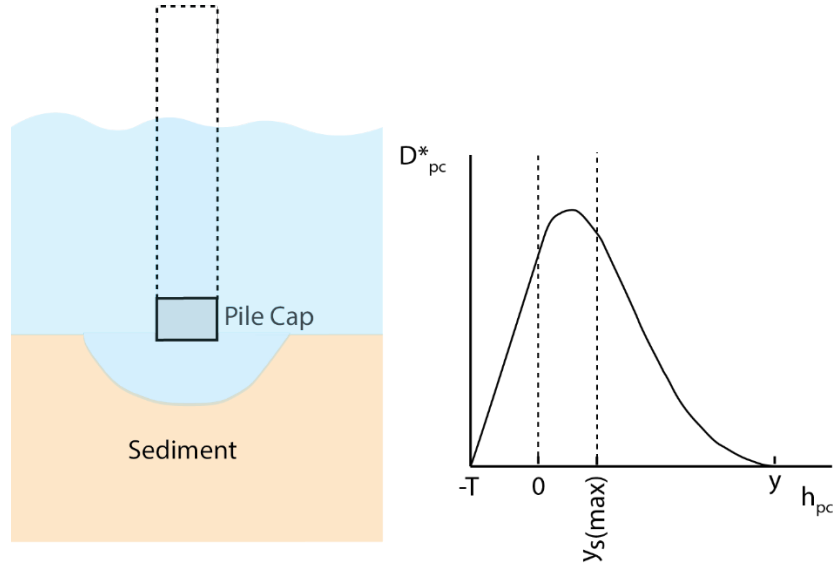
Figure 4-10 Sketch showing how the pile cap effective diameter changes with vertical location.

$$
f_{pch} = \begin{cases} 0 & h_{pc} > y \\ 0.65\left[(y - h_{pc})/(y - y_{s(max)}) \right]^2 & y_{s(max)} \le h_{pc} \le y \\ 1 - 0.35(h_{pc}/y_{s(max)})^2 & 0 \le h_{pc} < y_{s(max)} \\ 1 & h_{pc} < 0 \end{cases}
$$
4.33

$$
h_{pcpT} \equiv h_{pc} + T
$$

$$
f_{pchT} = \begin{cases} 0 & h_{pcpT} > y \\ 0.65\left[(y - h_{pcpT})/(y - y_{s(max)}) \right]^2 & y_{s(max)} \le h_{pcpT} \le y \\ 1 - 0.35(h_{pcpT}/y_{s(max)})^2 & 0 \le h_{pcpT} < y_{s(max)} \\ 1 & h_{pcpT} < 0 \end{cases}
$$
4.34

$$
K_{pch} = f_{pch} - f_{pchT}
$$
4.35

4.5.2. Pile Cap Length to Width Factor

The equations used to compute the effect of the pile cap length to width ratio is the same as that for the column (Eqs. 4.22-4.26) with the column parameters replaced by those for the pile cap, e.g.,

$$
LOB_{pc} = \frac{L_{pc}}{b_{pc}}, \text{ etc.}
$$

$$K_{LOBpc} = (f_{lob\_pc})(f_{hpc})$$ 4.36

4.6. Pile Group Effective Diameter

The effective diameter of the pile group is a function of the size and number of piles, their spacing, the height of the piles in the flow and their orientation to the flow.

$$D_{pg}^* \equiv K_{pgs} K_{pgpe} K_{pgh}$$ 4.37

4.6.1. Pile Group Shape Factor

The pile group shape factor is the same as that for the vertical datum calculations and equal to 1.4.

4.6.2. Pile Group Projection Factor

The refined projection factor is more complex and includes actual projections of some of the piles as well as the projection of the solid produced by setting the spacing between the piles to zero.

$K_{pgpe} \equiv$ the effective projection of the pile group

$K_{pgp} \equiv$ the actual projection of the first row and leading-edge column piles on a plane normal to the flow. For the 3 x 4 pile group in Fig. 4-11, $K_{pgp} = x1 + x2 + x3$
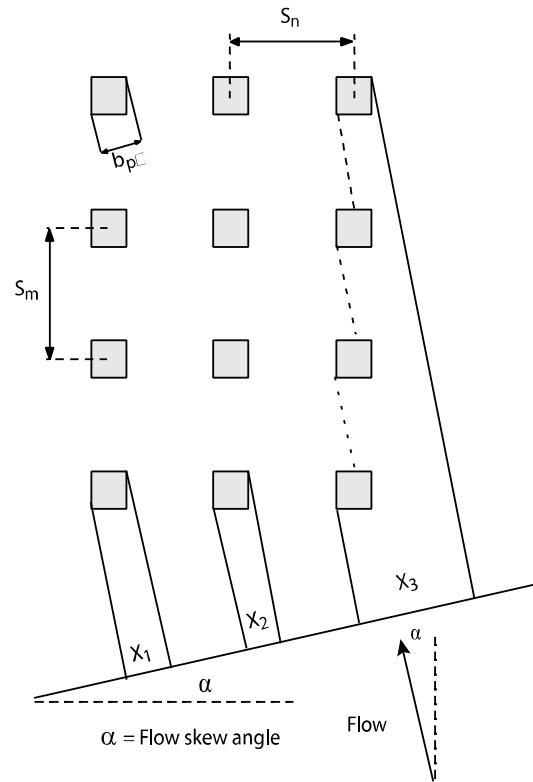
Figure 4-11 Sketch showing the pile group projection onto a vertical plane normal to the flow.

$K_{pgp1} \equiv$ projection of the pile group with zero spacing between the piles (see Fig. 4-12).
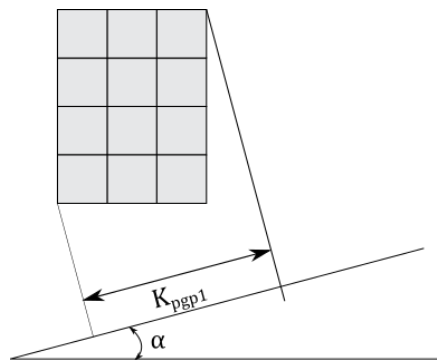
Figure 4-12 Projection of 3 x 4 pile group with zero spacing between piles.

The spacing, C_s, of the piles that result in the piles acting as individual piles (for scour computation purposes) is estimated using Eq. 4.38:

$$C_s = \begin{cases} -8.4\alpha/\pi + 9.3 & n = 1, m > 1 \\ 8.4\alpha/\pi + 5.1 & n > 1, m = 1 \\ 9.3 & n > 1, m > 1 \end{cases}$$ 4.38

Pile spacing used in the computations is as follows:

$$s = \begin{cases} s_n & s_n \le s_m \\ s_m & s_m \le s_n \end{cases}$$ 4.39

$s_n \equiv$ centerline spacing for piles perpendicular to the non-skewed flow
$s_m \equiv$ centerline spacing for piles inline with the non-skewed flow

The pile spacing is normalized by the projected width of a single pile.

$$soa = s/b_p$$ 4.40

where b_p is the projection of a single, unobstructed pile.

$$b_p = \begin{cases} b & 0 \le \alpha \le \pi/2 & \text{circular pile} \\ b[\cos(\alpha) + \sin(\alpha)] & 0 \le \alpha \le \pi/2 & \text{square pile} \end{cases}$$ 4.41

The effective diameter of the pile group that includes the effects of pile spacing is estimated by equations below.

$$f_a = C_s(K_{pgp} - b_p)/[(C_s - 1)K_{pgp}]$$
$$f_b = (C_s b_p - K_{pgp1})/[(C_s - 1)K_{pgp}]$$ 4.42

$$K_{pgpe} = K_{pgp}(f_a/soa + f_b)$$ 4.43

4.6.3. Vertical Position Factor

The vertical location of the top of the piles is also important in estimating the effective diameter of the pile group. Eq. 4.44 determines its influence:

$$K_{pgh} = \begin{cases} 1 & h_{pg} > y \\ 1 - 0.65 \left[(y - h_{pg})/(y - y_{s(max)}) \right]^2 & y_{s(max)} \le h_{pg} \le y \\ 0.35 \left(h_{pg}/y_{s(max)} \right) & 0 \le h_{pg} < y_{s(max)} \\ 0 & h_{pg} < 0 \end{cases} \qquad 4.44$$

4.7. Complex Structure Scour

Substituting the effective diameter D_{CS}^* of the complex structure along with the sediment properties and flow conditions of interest into Eqs. 3.4 – 3.11 yields the equilibrium local scour depth, $y_{s(complex\ structure)}$, at the complex structure for the specified sediment and flow parameters. However, a final correction is required. Due to the empirical nature of the equations and linear superposition assumptions, $y_{s(complex\ structure)}$ might not uncover the top of the pile cap even though pile cap scour is calculated. In this case the $y_{s(complex\ structure)}$ is corrected as follows:

$$y_{s(complex\ structure)} = \begin{cases} \max \left(y_{s(complex\ structure)}, -SF^* \left(h_{col} - y_{s(max)} \right) \right) & D_{pc}^* > 0 \\ y_{s(complex\ structure)} & D_{pc}^* = 0 \end{cases} \qquad 4.45$$

This scour depth is the maximum depth at some location at the base of the structure, usually, but not always, near the leading edge. In general, the bed level reduction for the remainder of the structure will be less.

4.8. Comparison with Data

Significant amounts of complex pier data became available in the literature since the last version of FDOT Scour Manual. Baghbadorani et al. (2018) collected 529 data points for complex piers. As a part of this study, this data set was augmented with additional data creating a data set with 908 unique measurements. The sources of this data are summarized in Table 4-1 and the ranges of data parameters are given in Table 4-2 and Table 4-3. The number of data points might not match the original data sets, because repetitions were removed. The quality of the different data sets varies significantly. The most significant source of error is the test duration, which varies from 3 hours to

more than a month. In fact, some studies do not report the experiment duration. This study employed the reported equilibrium scour from the data sets. Some data sets reported the scour at the end of the experiment as equilibrium scour. For short duration tests, the scour is under-reported. Other data sets extrapolated the final scour at the end of their experiment to yield an equilibrium scour. Depending on the methodology this might create under- and over-reporting errors. As a result, a large scatter should be expected in any kind of model prediction.

Table 4-1   Sources of Complex Pier Data Set

Data Source	Number of Measurements
(Amini et al. 2014)	51
(Ataie-Ashtiani et al. 2010)	71
(Baghbadorani et al. 2018)	52
(Beheshti and Ataie-Ashtiani 2016)	1
(Coleman 2005)	22
(Eghbali et al. 2013)	9
(Ferraro et al. 2013)	21
(Jones et al. 1992)	18
(Kothyari and Kumar 2012)	6
(Kumar and Kothyari 2012)	2
(Lança et al. 2013)	75
(Lu et al. 2011)	11
(Martin-Vide et al. 1998)	27
(Melville and Raudkivi 1996)	67
(Moreno et al. 2017)	83
(Moreno et al. 2016)	116
(Moreno et al. 2015)	6
(Oliveto 2012)	8
(Oliveto et al. 2006)	8
(Oliveto et al. 2004)	21
(Parola et al. 1996)	23
(Ramos et al. 2016)	1
(Sheppard 2005)	7
(Sousa and Ribeiro 2019)	12
(Umeda et al. 2010)	6
(Veerappadevaru et al. 2011)	6
(Yang et al. 2018)	84
(Yang et al. 2019)	94

Table 4-2 Summary of Dimensional Parameters for Laboratory Data Sets

Parameter	Minimum	Median	Mean	Maximum
y_0 (ft)	0.18	0.66	0.59	1.97
V (ft/s)	0.48	1.02	1.26	6.00
D_{50} (mm)	0.17	0.84	0.81	2.40
Skew (°)	0.00	0.00	7.01	90.00
b_{col} (ft)	0.03	0.15	0.19	0.56
b_{pc} (ft)	0.16	0.39	0.42	1.05
b_p (ft)	0.02	0.08	0.10	0.20
T (ft)	0.00	0.20	0.59	3.28
H_{pc} (ft)	-0.96	-0.10	-0.06	1.97
n	1	2	1.93	3
m	2	4	3.89	8

Table 4-3 Summary of Non-Dimensional Parameters for Laboratory Data Sets

Parameter	Minimum	Median	Mean	Maximum
Fr	0.14	0.23	0.32	1.85
V/V_c	0.56	0.86	1.14	5.68
b_{col}/y_0	0.05	0.30	0.34	2.14
b_{pc}/b_{col}	1.00	2.57	2.85	8.10
b_p/b_{pc}	0.08	0.21	0.23	0.50
T/y_0	0.00	0.45	1.00	8.17
H_{pc}/y_0	-1.00	-0.16	-0.13	1.00

The complex scour equations were developed employing a subset of this data set with 454 data points. These data points were chosen somewhat subjectively as being higher quality. However, the performance of the complex pier equations is evaluated employing the entire data set for completeness and transparency. Figure 4-13 through Figure 4-16 show the performance of different complex pier predictive equations: the new FDOT methodology with a safety factor (SF) of 1.25 (in Eq. 4.1), the new FDOT methodology with a safety factor of 1.00, the previous FDOT methodology, and HEC-18 Version 5 methodology, respectively. The new FDOT equations with a safety factor of 1.00 have much better predictive power than both the existing FDOT and HEC-18

equations. Notably, this study recommends employing a safety factor of 1.25 (SF=1.25) so that the equations effectively encapsulate the data (Figure 4-13).
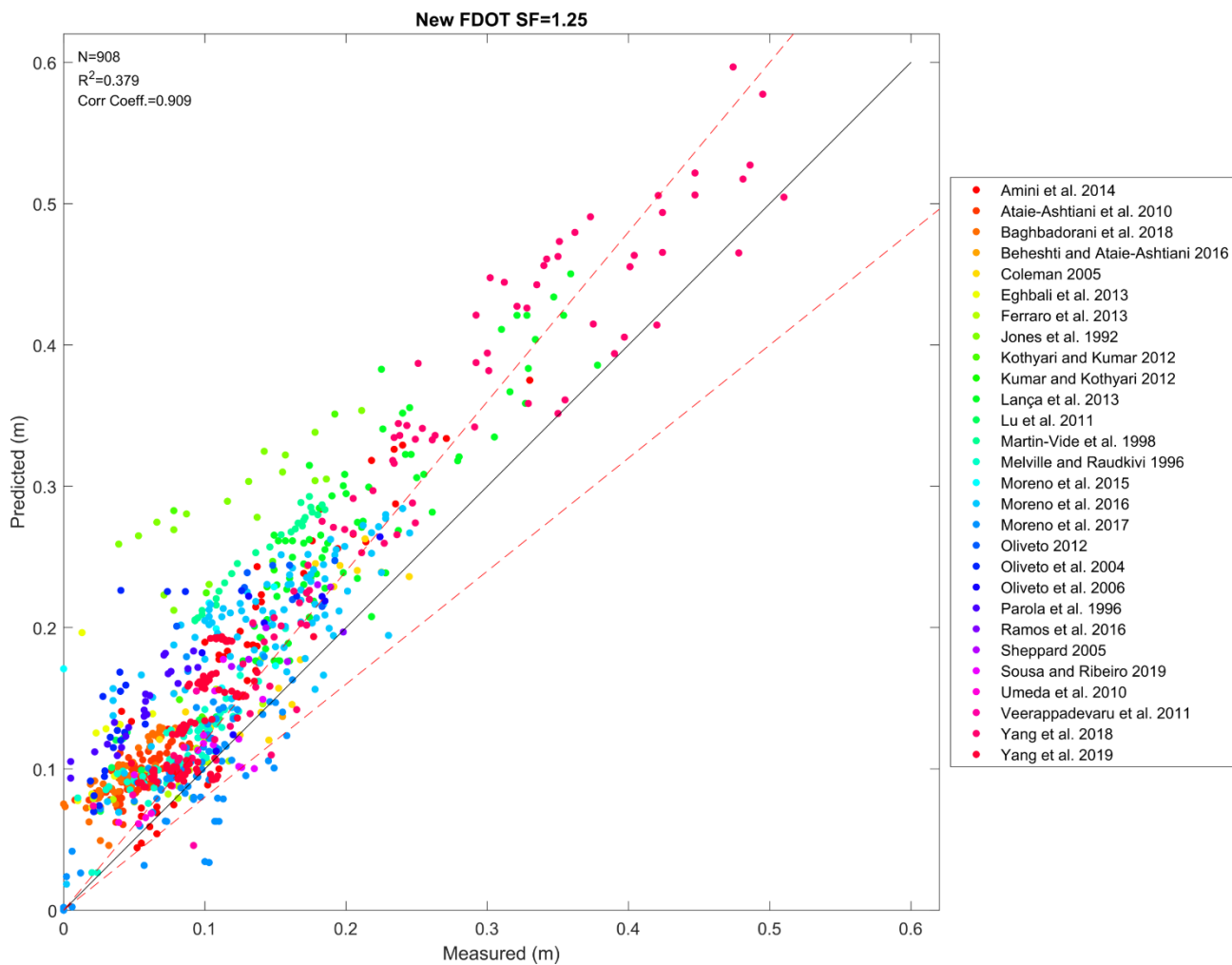

Figure 4-13 Performance of New FDOT Equations with Safety Factor=1.25
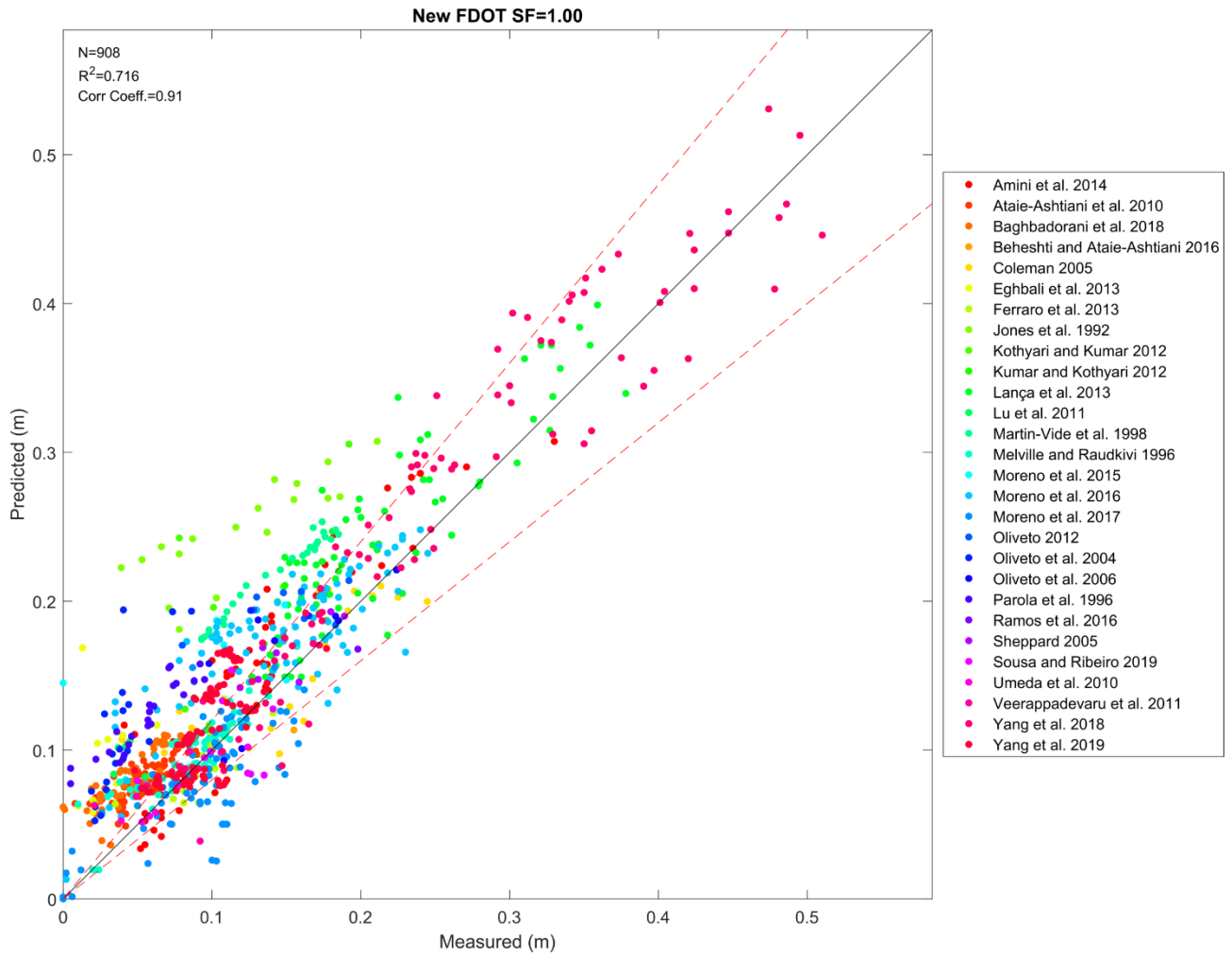
Figure 4-14 Performance of New FDOT Equations with Safety Factor=1.00
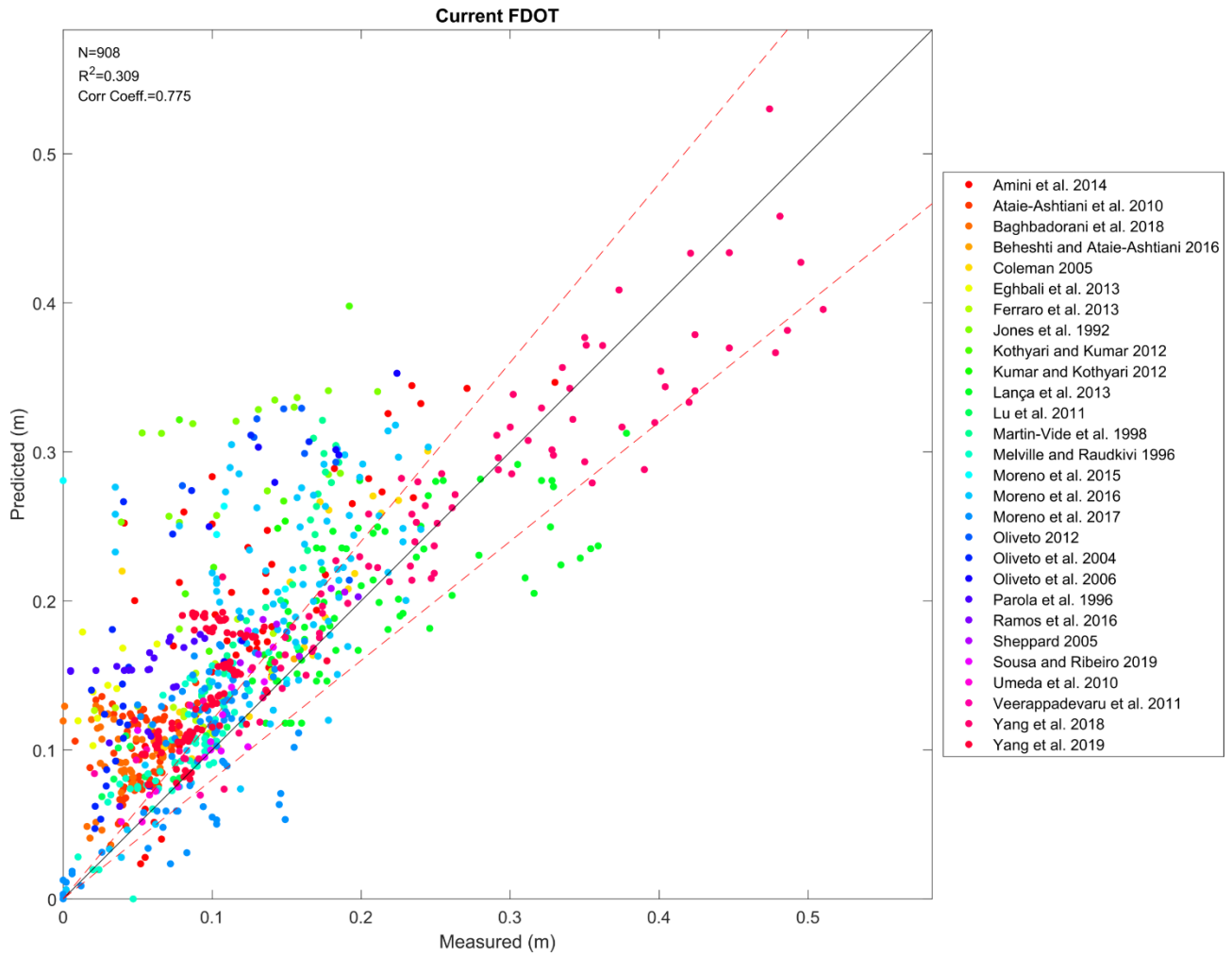
Figure 4-15 Performance of Current FDOT Equations
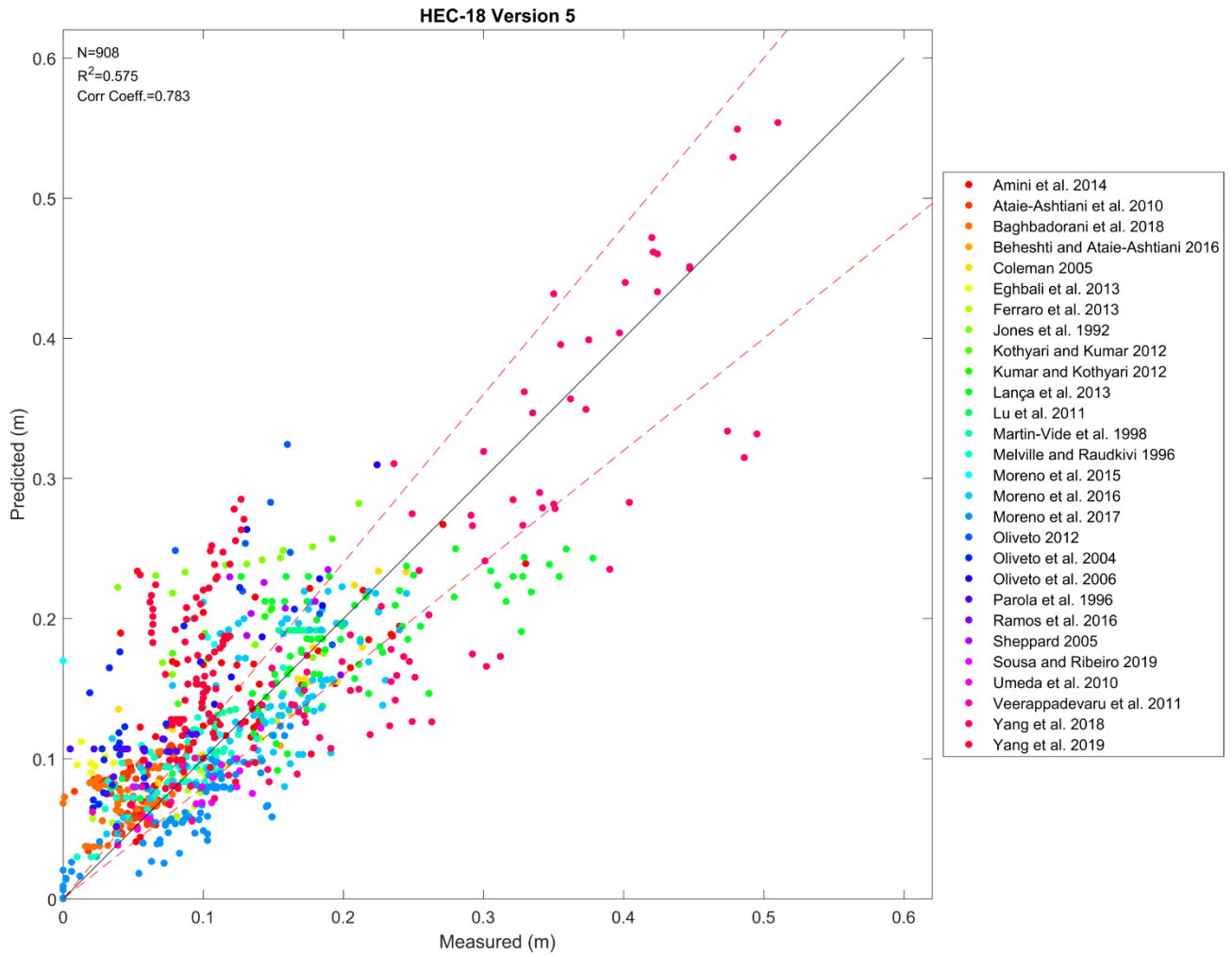
Figure 4-16 Performance of HEC-18 Version 5 Equations

CHAPTER 5 ADDITIONAL SCOUR RELATED ISSUES

Local sediment scour in cohesionless sediments, such as sand, has received the most attention by researchers and is perhaps the best understood and most accurately predicted. There are, however, other scour related topics of importance to practitioners and even though they are not as well understood are worthy of discussion. These topics include the impact of sediment gradation on equilibrium scour depths, the rate at which scour occurs, design scour depths in cohesive sediments and erodible rock, local scour at structures in close proximity to each other, etc. This chapter gives a brief description of some of these topics and indicates how they will most likely impact equilibrium scour depths. In some cases, procedures have been developed for obtaining conservative design scour depth predictions that are significantly less than those produced by previous methods.

5.1. Sediment Size Distribution

Laboratory experiments show [see e.g., Ettema (1976)] that the greatest local scour depths occur for uniform diameter sediments. For this reason, most researchers conduct their experiments with near uniform sediments (i.e., sediments with low values of sigma, $\sigma = \sqrt{D_{84} / D_{16}}$). The empirical scour prediction equations in Chapter 3 are based on data from laboratory experiments with near uniform diameter sediments. Sediments encountered at bridge crossings will always have a distribution of sediment sizes and thus will experience smaller scour depths than predicted by these equations. This is due to "armoring" of the scour hole by the larger particles left behind as the smaller particles are removed. In effect, the median grain size increases as the scour progresses, resulting in a lower value of V / V_c. It should be pointed out that the level of conservatism decreases as the value of V / V_c increases. That is, the larger the design flow velocity the less sensitive the equilibrium scour depth is to changes in grain size distribution. Figure 5-1 illustrates the work of Ettema (1976) in quantifying the effects of σ on equilibrium scour depths. K_σ is a multiplier that decreases the equilibrium scour depth with increasing values of σ. At the present time it is not recommended that design scour depth predictions be altered to account for sediment gradation for the sediment conditions in Florida. This effect does, however, provide some additional conservatism to the design scour prediction.
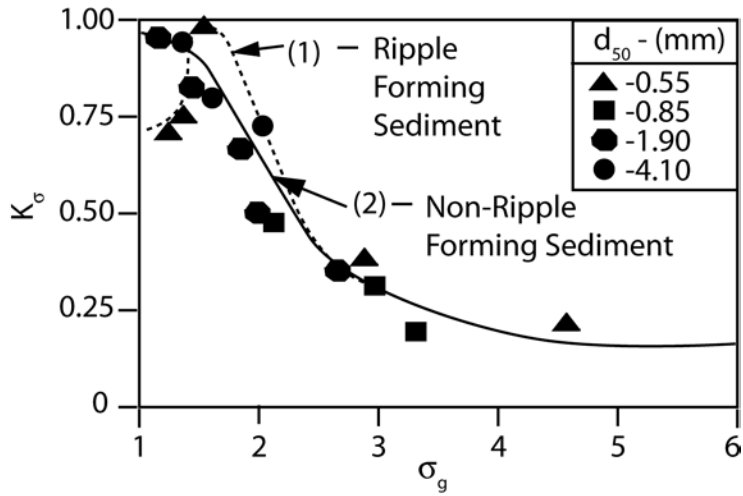
Figure 5-1 Effects of sediment size distribution, σ, on equilibrium scour depths.

5.2. Time Dependency of Local Scour

When a structure located in an erodible bed is subjected to a steady current, the rate of local scour is large at first, but then decreases as the scour hole deepens. The time required to reach an equilibrium scour depth for a given structure, sediment and flow situation is not well understood; especially in the high velocity, live-bed scour range. For many coastal locations where the design storm event results from hurricane storm surge generated currents, the duration of the event may not be sufficient to achieve equilibrium scour conditions. This is particularly true if the sediment contains cohesive materials. Thus, employing equations that predict equilibrium scour depths will produce conservative values, if the time to reach equilibrium scour depths is not taken into consideration.

A recent NCHRP study investigated published equations/methods for predicting local scour evolution rates. The best performing methods were modified to improve their performance with laboratory data from several sources. The resulting most accurate equation, referred to as the Melville/Sheppard equation, is presented below. This form of the equation has not been published and thus must be applied with caution and sound engineering judgment. The investigators could not locate any data for scour evolution rates at large structures subjected to high velocity flows with which to test the equations. For this reason, a safety factor of one (1) is recommended for scour rates in the clear-water range and one-half (0.5) in the live-bed range. Note that the safety factor is on the reference time t_e and a value of less than 1.0 reduces the time to reach equilibrium and thus yields a more conservative value. With these safety factors the predictions are thought to be

57

conservative (i.e., the predicted rates are greater than anticipated).

The Melville/Sheppard equation is presented below. Notably, these equations are provided for reference to demonstrate the level of conservatism when employing steady state derived scour predictions to an unsteady process. At this time, the FDOT does not recommend employing time dependent scour predictions for design.

$$y_{st}(t) = K_t y_s$$

$$K_t = \exp\left\{C_1 \left| \frac{V_c}{V} \ln\left(\frac{t}{t_e}\right) \right|^{1.6}\right\}$$

$$t_e(\text{days}) = SF\, C_2 \frac{D^*}{V}\left(\frac{V}{V_c} - 0.4\right) \qquad\qquad \frac{y_0}{D^*} > 6, \quad \frac{V}{V_c} > 0.4$$

$$t_e(\text{days}) = SF\, C_3 \frac{D^*}{V}\left(\frac{V}{V_c} - 0.4\right)\left(\frac{y_0}{D^*}\right)^{0.25} \qquad \frac{y_0}{D^*} \le 6, \quad \frac{V}{V_c} > 0.4$$

$$t_{90}(\text{days}) = \exp(-1.83\frac{V}{V_c})t_e$$

where
$y_{st}(t)$ = time dependent local scour depth,
y_s = equilibrium scour equation using Eqs. 3-4 through 3-13,
$C_1 = -0.04$,
$C_2 = 200$ days/s,
$C_3 = 127.8$ days/s,
SF =1.0 for clear-water scour and 0.5 for live-bed scour ($V/V_c > 1.0$)
t_e = reference time
t_{90} = time to reach 90% of equilibrium scour depth
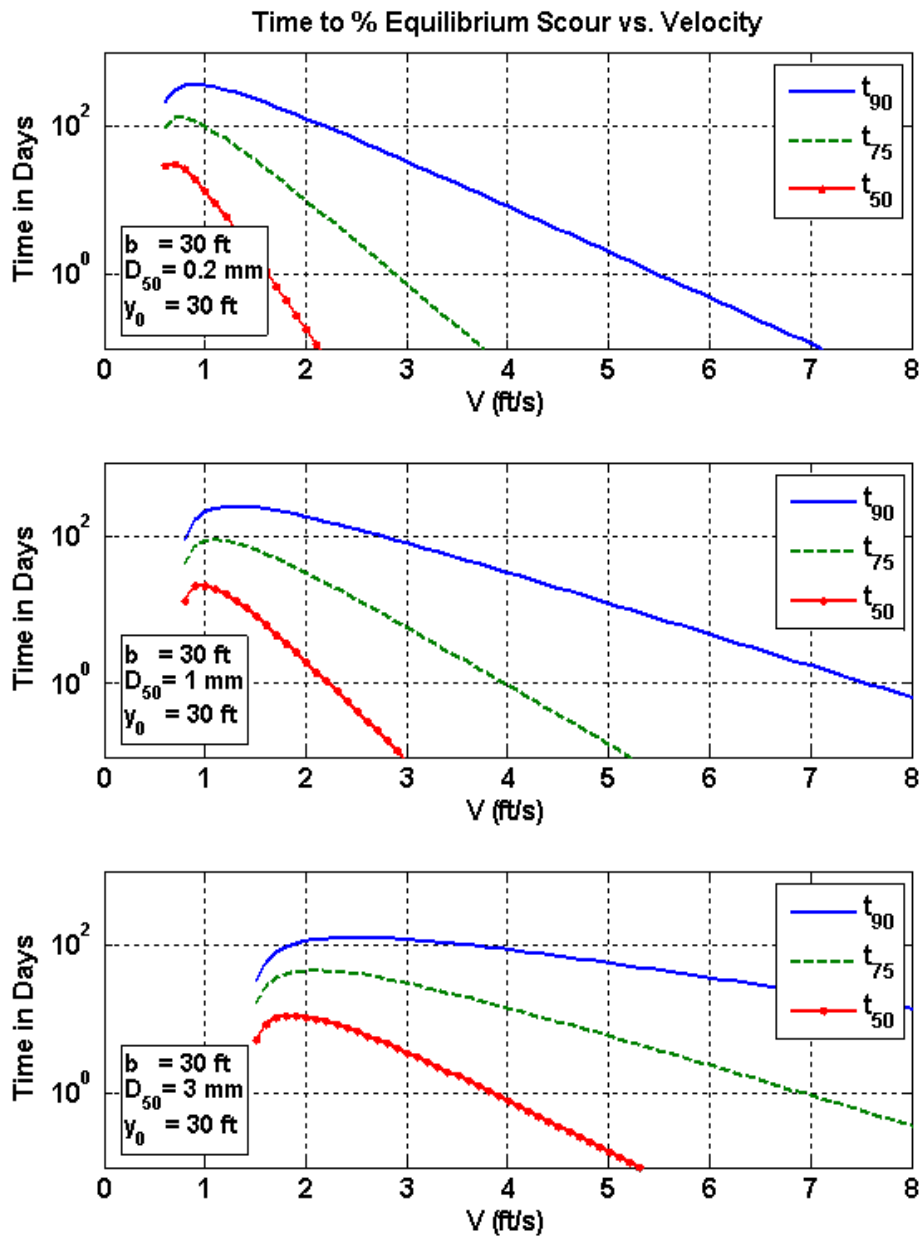
Figure 5-2   Example plots of time to reach three different percents of equilibrium scour depths as functions of flow velocity and sediment grain size, for a single circular pier. The safety factor, SF, is equal to 1.0 in these plots.

5.3. Scour in Sediments Other than Sand

The erosion properties of sediments other than sand (and other cohesionless materials) can be highly variable. For this reason, these materials have been treated as sand when computing design equilibrium scour depths for bridge foundations. The University of Florida under contract to the Florida Department of Transportation developed procedures and testing equipment for predicting design scour depths in these sediments. These methods require that sediment samples from the site be taken and tested to determine their rate of erosion as a function of water flow induced shear stress. Two apparatus were developed for the purpose of obtaining the erosion rate information. One apparatus, the "Rotating Erosion Test Apparatus" or RETA is best suited for erodible rock materials. The second apparatus the "Sediment Erosion Rate Flume" or SERF is better suited for clays, sand-clay mixtures, silts, etc. The FDOT State Materials Laboratory in Gainesville, FL has five operating RETAs. The only SERF unit was located in a Civil Engineering Laboratory at the University of Florida but was recently disassembled and awaiting reassembly at the University of North Florida. Photographs of the RETA and SERF are shown in Figure 5-3 and Figure 5-4, respectively.
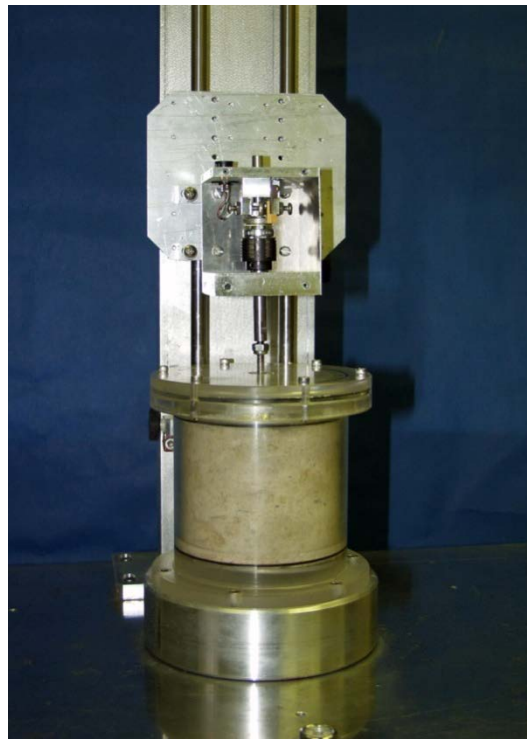
Figure 5-3   Rotating Erosion Test Apparatus (RETA). The Florida Department of Transportation State Materials Laboratory currently has five operating RETAs.

Figure 5-4   Sediment <u>E</u>rosion <u>R</u>ate <u>F</u>lume (SERF) located in a Civil Engineering Laboratory at the University of Florida.

The RETAs require cylindrical intact samples greater than 4 inches in length and either 2.4 or 4.0 inches in diameter. These are two of the standard rock core diameters. Sediment samples taken with Shelby Tubes with outside diameters up to 2.875 inches can be tested in the SERF. Sediment sample lengths greater than 12 inches are preferred. Tests are performed in both apparatus at different shear stresses and plots of rate of erosion versus shear stress are produced. This information along with projected daily flow rates (including magnitude and frequency of storm flow events) at the site for the life of the structure are used to obtain design contraction and local scour depths.

When erodible rock is encountered at a bridge site and design scour depths are required, the appropriate FDOT District Drainage Engineer and/or the State Hydraulics Engineer should be contacted regarding having core samples tested at the FDOT State Materials Laboratory in Gainesville, FL. The test results should then be analyzed to establish design scour depths.

5.4. Local Scour at Piers in Close Proximity to other Piers

Often, a roadway crossing of a water body involves two bridges conveying traffic in both directions. In many of these cases the piers on the bridges are in close proximity to each other. This influences the flow, turbulence, and bed shear stresses in the vicinity of the piers and complicates local scour prediction. The best solution for this problem is to conduct a physical model study with model piers. When physical model studies are conducted, care must be taken when computing scour depths at the prototype piers from the model study results. The predictive equations for single piers presented in Chapter 3 can account for scale effects. Basically, the physical model tests can determine the effective diameter of the two-structure model, D^*_{model}, from which the effective diameter of the prototype piers can be computed employing the geometric scale of the model. That is, if a 1:20 scale model is used the prototype effective diameter, $D^*_{prototype}$ is simply 20 times the effective diameter of the two pier models. Once $D^*_{prototype}$ is known for the combined prototype structures, the equations in Chapter 3 can estimate the scour depth for the prototype sediment and flow conditions. If the piers in question have complex geometries, as discussed in Chapter 4, then the flow rates and sediment employed in the model tests must be adjusted such that the anticipated portions of the structure exposed to the flow in the prototype during the scouring process are replicated in the model tests. The procedure outlined below for computing approximate scour depths at multiple, close proximity, structures will be helpful in estimating how much of a partially buried or buried pile cap will be exposed during a design flow event. If it is not possible to conduct physical model tests, then the method described below can estimate the local scour depth. If, however, the bridge in question is critical then a physical model test is recommended. The following concept for estimating scour depths at two or more structures in close proximity has had only minimal testing. The few tests that were conducted did, however, yield conservative, but acceptable results.

Consider the two complex piers shown in plan view in Figure 5-5. Application of the equations presented in Chapter 4 can provide the effective diameter of each individual pier. These effective diameters are shown below the piers in Figure 5-5. Note that in the figure one effective diameter is larger than the other due to the pier size being larger. The next step is to treat the two effective diameters as two piles in a pile group and apply the equations for scour at pile groups in Chapter 4 to compute the scour. However, these equations were developed for piles of equal size and that is

not the case in this situation. A conservative assumption would be to increase the diameter of the smaller pile to that of the larger, provided the difference in the two is not too large (e.g., if the smaller diameter is greater than 70% of the larger). Computing the scour depth for the pile group with two equal diameter piles will yield a conservative estimate of the maximum scour depth at the two complex piers for the specified sediment and flow conditions.
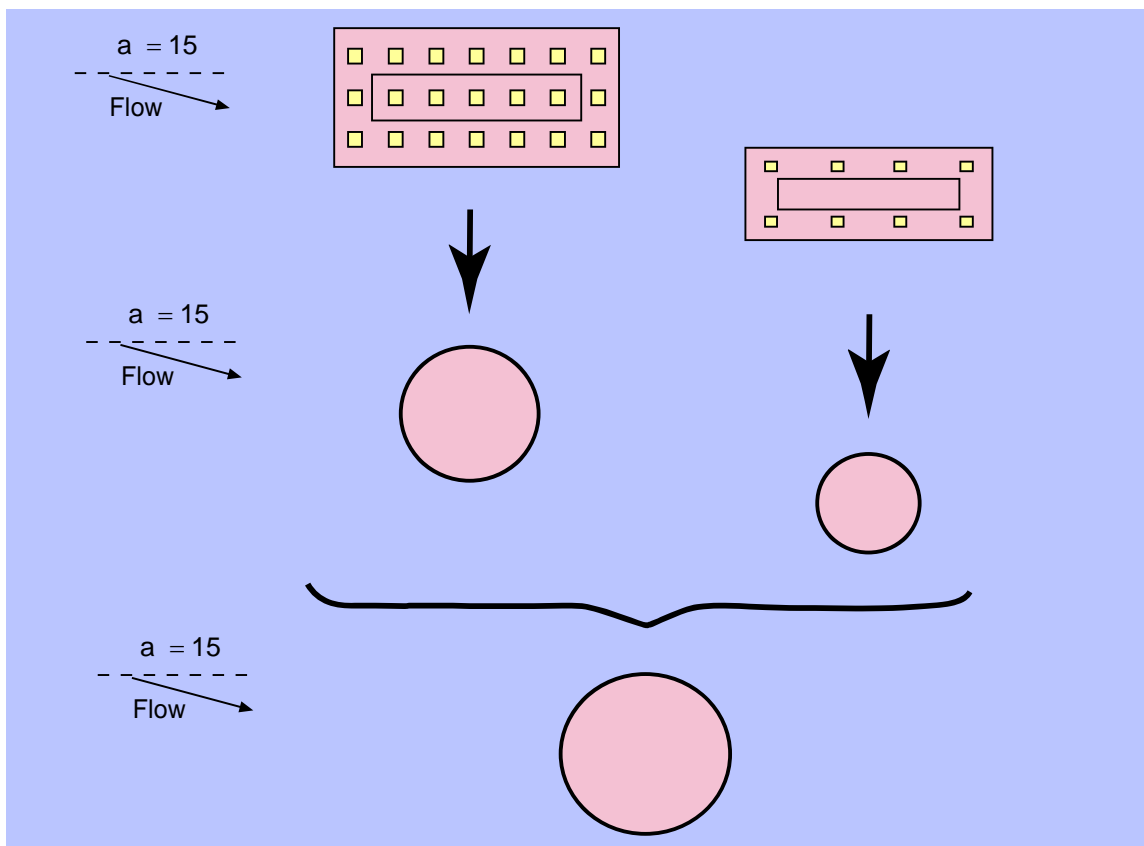

Figure 5-5   Definition sketch for estimating local scour depths at piers in close proximity to each other.

BIBLIOGRAPHY

Agaccioglu, H., and Onen, F. (2005). "Clear-water scour at a side-weir intersection along the bend." Irrig. Drain., 54(5), 553-569.

Ahmad, M. (1953). "Experiments on design and behavior of spur dikes." In: International Hydraulics Convention, St. Anthony Falls Hydraulics Laboratory, Minneapolis, MN,, 149-159.

Ahmad, M. (1962). "Discussion of 'Scour at Bridge Crossings' by EM Laursen." Trans. of ASCE, 127, pt. I(3294), 198-206.

Allen, J. R. L. (1976). "Computational Models for Dune Time-Lag: General Ideas, Difficulties, and Early Results." Sedimentary Geology, 16, 255-279.

Annandale, G. W. (2000). "Prediction of scour at bridge pier foundations founded on rack and other earth materials." In: Fifth International Bridge Engineering Conference, Vols 1 and 2, Transportation Research Board Natl Research Council, Washington, A67-A70.

Arneson, L.A., Zevenbergen, L.W., Lagasse, P.F., Clopper, P.E. (2012). "Evaluating scour at bridges. Fifth Edition." Hydraulic Engineering Circular No. 18 (HEC-18), Federal Highway Administration, Washington D.C

Ataie-Ashtiani, B., and Beheshti, A. A. (2006). "Experimental investigation of clear-water local scour at pile groups." J. Hydraul. Eng.-ASCE, 132(10), 1100-1104.

Babaeyan-Koopaei, K. (2003). "Flow pattern in the scour hole around a cylinder - By Graf, W.H. and Istiarto, I., Journal of Hydraulic Research, volume 40, 2002, issue 1, pp. 13-20." Journal of Hydraulic Research, 41(4), 443-446.

Baker, R. E. (1986). "Local Scour at Bridge Piers in Non-uniform Sediment." University of Auckland, Auckland, New Zealand.

Barbhuiya, A. K., and Dey, S. (2004). "Local scour at abutments: A review." Sadhana-Acad. Proc. Eng. Sci., 29, 449-476.

Barkdoll, B. S. (2000). "Time scale for local scour at bridge piers - Discussion." J. Hydraul. Eng.-ASCE, 126(10), 793-794.

Basak, V. (1975). "Scour at Square Piers." Devlet su isteri genel mudulugu, Ankara, Turkey.

Beheshti, A.-A., and Ataie-Ashtiani, B. (2016). "Scour hole influence on turbulent flow field around complex bridge piers." Flow. Turbulence and Combustion, 97(2), 451–474.

Blench, T. (1962). "Discussion of 'Scour at bridge crossings' by E.M. Laursen." Trans. of ASCE, 127, pt. I(3294), 180-183.

Bonasoundas, M. (Year). "Non-stationary Hydromorphological Phenomena and Modelling of Scour Process." 16th IAHR Congress, Sao Paulo, Brazil, 9-16.

Boon, J. H. d., Sutherland, J., Whitehouse, R., Soulsby, R., Stam, C. J. M., Verhoeven, K., Høgedal, M., and Hald, T. (2004). "Scour Behaviour and Scour Protection for Monopile Foundations of Offshore Wind Turbines." In: Wind Energy Conference, London, UK.

Breusers, H. N. C., Nicollet, G., and Shen, H. W. (1977). "Local Scour Around Cylindrical Piers." Journal of Hydraulic Research, 15(3), 211-252.

Briaud, J. L., Chen, H. C., Kwak, K. W., Han, S. W., and Ting, F. C. K. (2001). "Multiflood and multilayer method for scour rate prediction at bridge piers." J. Geotech. Geoenviron. Eng., 127(2), 114-125.

Chabert, J., and Engeldinger, P. (1956). "Étude des affouillements autour des piles de ponts." Laboratoire National d'Hydraulique, Chatou, France (in French).

Chang, W. Y., Lai, J. S., and Yen, C. L. (2004). "Evolution of scour depth at circular bridge piers." J. Hydraul. Eng.-ASCE, 130(9), 905-913.

Chiew, Y. M. (1984). "Local Scour at Bridge Piers." Report No 355, Dept. of Civil Eng. Auckland Univ, Auckland New Zealand.

Chiew, Y. M. (2000). "Time scale for local scour at bridge piers - Closure." J. Hydraul. Eng.-ASCE, 126(10), 794-795.

Chiew, Y. M. (2004). "Local scour and riprap stability at bridge piers in a degrading channel." J. Hydraul. Eng.-ASCE, 130(3), 218-226.

Chitale, S. V. (1962). "Scour at bridge crossings." Transactions of the American Society ofCivil Engineers, 127(1), 191-196.

Coleman, S. E. (2005). "Clearwater local scour at complex piers." J. Hydraul. Eng.-ASCE, 131(4), 330-334.

Coleman, S. E. (2005). "Clearwater Local Scour at Complex Piers." Journal of Hydraulic Engineering, 131(4), 330–334.

Coleman, S. E., and Melville, B. W. (2001). "Case study: New Zealand bridge scour experiences." J. Hydraul. Eng.-ASCE, 127(7), 535-546.

Coleman, S. E., Lauchlan, C. S., and Melville, B. W. (2003). "Clear-water scour development at bridge abutments ((((has discussion)))))))." Journal of Hydraulic Research, 41(5), 521-531.

Coleman, S. E., Lauchlan, C. S., Melville, B. W., and Giri, S. (2005). "Clear-water scour development at bridge abutments." Journal of Hydraulic Research, 43(4), 445-447.

Cunha, L. V. (1970). "Discussion of 'Local scour at bridge crossings' by Shen H.W., Schneider V.R. and Karaki S.S." Trans. of ASCE, 96(HY8), 191-196.

Davis, S. R., Shea, C., and Pagan-Ortiz, J. E. (2000). "Guideline for evaluation of scour at bridges - Proposed ASCE standard." In: Fifth International Bridge Engineering Conference, Vols 1 and 2, Transportation Research Board Natl Research Council, Washington, A64-A66.

Dean, R. G., and Dalrymple, R. A. (2002). Coastal Processes with Engineering Applications, Cambridge University Press.

den Boon, J. H., Sutherland, J., Whitehouse, R., Soulsby, R., Stam, C. J. M., Verhoeven, K., Høgedal, M., and Hald, T. (Year). "Scour Behaviour and Scour Protection for Monopile Foundations of Offshore Wind Turbines." Proceedings 2004 European Wind Energy Conference, European Wind Energy Association, London, UK, 14.

Dey, S., and Barbhuiya, A. K. (2004). "Clear water scour at abutments." Proc. Inst. Civil. Eng.-Water Manag., 157(2), 77-97.

Dey, S., and Barbhuiya, A. K. (2004). "Clear-water scour at abutments in thinly armored beds." J. Hydraul. Eng.-ASCE, 130(7), 622-634.

Dey, S., and Barbhuiya, A. K. (2005). "Time variation of scour at abutments." J. Hydraul. Eng.-ASCE, 131(1), 11-23.

Dey, S., and Barbhuiya, A. K. (2005). "Turbulent flow field in a scour hole at a semicircular abutment." Can. J. Civ. Eng., 32(1), 213-232.

Dey, S., and Barbhuiya, A. K. (2006). "3D flow field in a scour hole at a wing-wall abutment." Journal of Hydraulic Research, 44(1), 33-50.

Dey, S., and Barbhuiya, A. K. (2006). "Velocity and turbulence in a scour hole at a vertical-wall abutment." Flow Meas. Instrum., 17(1), 13-21.

Dey, S., and Raikar, R. V. (2005). "Scour in long contractions." J. Hydraul. Eng.-ASCE, 131(12), 1036-1049.

Dey, S., and Raikar, R. V. (2007). "Characteristics of horseshoe vortex in developing scour holes at piers." J. Hydraul. Eng.-ASCE, 133(4), 399-413.

Dey, S., and Raikar, R. V. (2007). "Clear-water scour at piers in sand beds with an armor layer of gravels." J. Hydraul. Eng.-ASCE, 133(6), 703-711.

Diab, R. (2011). "Experimental Investigation on Scouring around Piers of different Shape and Alignment in Gravel," PhD Dissertation, Darmstadt University of Technology.

Eghbali, P., Dehghani, A., Arvanaghi, H., and Menazadeh, M. (2013). "The effect of geometric parameters and foundation depth on scour pattern around bridge pier." Journal of Civil Engineering and Urbanism, Citeseer, 3(4), 156–163.

Ettema, R. (1976). "Influence of bed material gradation on local scour," Master's Thesis, University of Auckland, Auckland, New Zealand.

Ettema, R. (1980). "Scour at Bridge Piers." Report No 216, University of Auckland.

Ettema, R. (2001). "A Framework for Investigating Micro-models." The University of Iowa, Iowa City.

Ettema, R., Kirkil, G., and Muste, M. (2006). "Similitude of large-scale turbulence in experiments on local scour at cylinders." J. Hydraul. Eng.-ASCE, 132(1), 33-40.

Fael, C. M. S., Simarro-Grande, G., Martin-Vide, J. P., and Cardoso, A. H. (2006). "Local scour at vertical-wall abutments under clear-water flow conditions." Water Resour. Res., 42(10), 12.

Farrag, K., and Morvant, M. (2001). "Development of database for Louisiana highway bridge-scour data." In: Geology and Properties of Earth Materials 2001, Transportation Research Board Natl Research Council, Washington, 34-40.

Federico, F., Silvagni, G., and Volpi, F. (2003). "Scour vulnerability of river bridge piers." J. Geotech. Geoenviron. Eng., 129(10), 890-899.

Ferraro, D., Tafarojnoruz, A., Gaudio, R., and Cardoso, A. H. (2013). "Effects of Pile Cap Thickness on the Maximum Scour Depth at a Complex Pier." Journal of Hydraulic Engineering, 139(5), 482–491.

Fredsoe, J. (1980). "The formation of Dunes." International Symposium on River Sedimentation, Beijing, China.

Froehlich, D. C. (1988). "Analysis of Onsite Measurements of Scour at Piers." In: ASCE National Hydraulic Engineering Conference, ASCE, Colorado Springs, Colorado, 534-539.

Gao, D., Posada, G. L., and Nordin, C. F. (1993). "Pier scour equations used in the Peoples Republic of China." FHWA-SA-93-076, Washington, D.C.

Garde, R. J., Ranga Raju, K. G., and Kothyari, U. C. (1993). Effect on unsteadiness and stratification on local scour, International Science Publisher, New York.

Graf, W. H., and Istiarto, I. (2002). "Flow pattern in the scour hole around a cylinder." Journal of Hydraulic Research, 40(1), 13-20.

Graf. (1995). "Load scour around piers." Annual Report., Laboratoire de Recherches. Hydrauliques, Ecole Polytechnique Federale de Lausanne, Lausanne, Switzerland, pp. B.

Grimaldi, C. (2005). "Non-conventional countermeasures against local scouring at bridge piers," PhD Dissertation, Universita della Calabria.

Grimaldi, C., Gaudio, R., Cardroso, A., and Calomino, F. (2006). "Local scouring at bridge piers and abutments: Time evolution and equilibrium." In: Proc., River Flow 2006, Lisbon, Portugal, 1657-1664.

Gust, G. (1976). "Observations on turbulent-drag reduction in a dilute suspension of clay in sea-water." J. Fluid Mech, 75(1), 29-47.

Han, Y. F., and Chen, Z. C. (2004). "Experimental study on local scour around bridge piers in tidal current." China Ocean Eng., 18(4), 669-676.

Hancu, S. (Year). "Sur le calcul des affouillements locaux dans la zone des piles des ponts." 14th International Association of Hydraulic Research Congress, Paris, France, 299-313.

Hannah, C. R. (1978). "Scour at pile groups," University of Canterbury, Christchurch, New Zealand.

Harmsen, P., Palmer, R., and Turkiyyah, G. (2001). "Development and application of an expert system for evaluation of scour and stream stability." Civ. Eng. Environ. Syst., 18(3), 171-192.

Harris, J. M., Herman, W. M., and Cooper, B. S. (2004). "Offshore wind farms-an approach to scour assessment." In: Second Int. Confernce on Scour and Erosion, Singapore, 283-291.

Inglis, S. C. (1949). "Maximum depth of scour at heads of guide banks and groynes, pier noses, and downstream of bridges—The behavior and control of rivers and canals." Indian Waterways Experimental Station, Poona, India.

Jain, S. C., and Fischer, E. E. (1979). "Scour around bridge piers at high Froude numbers." FH-W A-RD- 79-104, Federal Highway Administration, U .S. Department of Transportation, Washington, D.C., U.S.A.

Jetté, C. D., and Hanes, D. M. (1997). "High-resolution sea-bed imaging: an acoustic multiple transducer array." Measurement Science and Technology, 8, 787-792.

Johnson, P. A., Hey, R. D., Tessier, M., and Rosgen, D. L. (2001). "Use of vanes for control of scour at vertical wall abutments." J. Hydraul. Eng.-ASCE, 127(9), 772-778.

Jones, J. S., and Sheppard, D. M. (2000). "Scour at Wide Bridge Piers. ." In: ASCE World Water Conference, , Minneapolis, MN. .

Jones, J. S., and Sheppard, D. M. (Year). "Local Scour at Complex Pier Geometries."

Jones, J. S., and Sheppard, D. M. (Year). "Scour at Wide Piers."

Jones, J. S., Kilgore, R. T., and Mistichelli, M. P. (1992). "Effects of Footing Location on Bridge Pier Scour." Journal of Hydraulic Engineering, 118(2), 280–290.

Kells, J. A., Balachandar, R., and Hagel, K. P. (2001). "Effect of grain size on local channel scour below a sluice gate." Can. J. Civ. Eng., 28(3), 440-451.

Kohli, A., and Hager, W. H. (2001). "Building scour in floodplains." Proc. Inst. Civil Eng.-Water Marit. Energy, 148(2), 61-80.

Korkut, R., Martinez, E. J., Morales, R., Ettema, R., and Barkdoll, B. (2007). "Geobag performance as scour countermeasure for bridge abutments." J. Hydraul. Eng.-ASCE, 133(4), 431-439.

Kothyari, U. C. (2007). "Indian practice on estimation of scour around bridge piers—A comment." Sadhana, 32(3), 187-197.

Kothyari, U. C., and Kumar, A. (2012). "Temporal variation of scour around circular compound piers." Journal of Hydraulic Engineering, American Society of Civil Engineers, 138(11), 945–957.

Kothyari, U. C., and Raju, K. G. R. (2001). "Scour around spur dikes and bridge abutments." Journal of Hydraulic Research, 39(4), 367-374.

Kothyari, U. C., Hager, W. H., and Oliveto, G. (2007). "Generalized approach for clear-water scour at bridge foundation elements." J. Hydr. Engng., in press.

Krishnamurthy, M. (1970). "Discussion of 'Local scour at bridge crossings' by Shen, H.W., Schneider, V.R. and Karaki, S.S." Trans. of ASCE, 96 (HY7), 1637-1638.

Kuhnle, R. A., Alonso, C. V., and Shields, F. D. (2002). "Local scour associated with angled spur dikes." J. Hydraul. Eng.-ASCE, 128(12), 1087-1093.

Kumar, A., and Kothyari, U. C. (2012). "Three-dimensional flow characteristics within the scour hole around circular uniform and compound piers." Journal of Hydraulic Engineering, American Society of Civil Engineers, 138(5), 420–429.

Lagasse, P. F., and Richardson, E. V. (2001). "ASCE compendium of stream stability and bridge scour papers." J. Hydraul. Eng.-ASCE, 127(7), 531-533.

Lagasse, P.F., Zevenbergen, L.W., Spitz, W.J., and Arneson, L.A. (2012). "Stream Stability at Highway Structures, Fourth Edition." Hydraulic Engineering Circular No. 20 (HEC-20), Federal Highway Administration, Washington D.C.

Lança, R., Fael, C., Maia, R., Pêgo, J. P., and Cardoso, A. H. (2013). "Clear-Water Scour at Pile Groups." Journal of Hydraulic Engineering, 139(10), 1089–1098.

Larras, J. (1963). "Profondeurs maximales d'erosion des fonds mobiles autour des piles enriviere." Ann. ponts et chaussées,, 133(4), 411-424.

Laursen, E. M. (1958). "Scour at bridge crossings." Iowa Highway Research Board, Ames, Iowa, U.S.A.

Laursen, E. M. (1962). "Scour at bridge crossings." Trans. of ASCE, 84(HY1), 166-209.

Laursen, E. M. (1963). "Analysis of relief bridge scour." Journal of the Hydraulics Division, 89(3), 93-118.

Laursen, E. M., and Toch, A. (1956). "Scour around bridge piers and abutments." Iowa Highway Research Board, State University of Iowa.

Lee, S., Sturm, T. W., Gotvald, A., and Landers, M. (Year). "Comparison of Laboratory and field measurements of bridge pier scour." Second Int. Conference on Scour and Erosion, Singapore, 231-239.

Li, H., Barkdoll, B. D., Kuhnle, R., and Alonso, C. (2006). "Parallel walls as an abutment scour countermeasure." J. Hydraul. Eng.-ASCE, 132(5), 510-520.

Li, Y., Wang, J., Wang, W., Briaud, J.-L., and Chen, H.-C. (2002). "Comparison Between Predictions and Measurements." In: First International Conference on Scour of Foundations, COLLEGE STATION, TEXAS, USA.

Link, O., and Zanke, U. (2004). "Influence of flow depth on scour at a circular pier in uniform coarse sand." In: Second Int. Confernce on Scour and Erosion, Singapore, 97-104.

Link, O., and Zanke, U. (2004). "On the time-dependent scour-hole volume evolution at a circular pier in uniform coarse sand." In: Second Int. Confernce on Scour and Erosion, Singapore, 207-214.

Lopez, G., Teixeira, L., Ortega-Sanchez, M., and Simarro, G. (2006). "Discussion of "Further results to time-dependent local scour at bridge elements" by Giuseppe Oliveto and Willi H. Hager." J. Hydraul. Eng.-ASCE, 132(9), 995-996.

Lu, J.-Y., Shi, Z.-Z., Hong, J.-H., Lee, J.-J., and Raikar, R. V. (2011). "Temporal variation of scour depth at nonuniform cylindrical piers." Journal of Hydraulic Engineering, American Society of Civil Engineers, 137(1), 45–56.

Martin-Vide, J. P., Hidalgo, C., and Bateman, A. (1998). "Local Scour at Piled Bridge Foundations." Journal of Hydraulic Engineering, 124(4), 439–444.

Mashahir, M. B., Zarrati, A. R., and Rezay, M. J. (Year). "Time development of scouring around a bridge pier protected by collar." Second Int. Confernce on Scour and Erosion, Singapore.

May, R. W. P., Ackers, J. C., and Kirby, A. M. (2002). "Manual on scour at bridges and other hydraulic structures." CIRIA Report C551.

May, R. W. P., and Escarameia, M. (2002). "Local Scour Around Structures in Tidal Flows." In: First International Conference on Scour of Foundations, COLLEGE STATION, TEXAS, USA.

Melville, B. W. (1975). "Local scour at bridge sites." University of Auckland, School of Engineering Report no. 117, Auckland, New Zealand.

Melville, B. W. (1984). "Live-bed scour at bridge piers." J. Hydraul. Eng.-ASCE, 110(9), 1234-1247.

Melville, B. W. (1997). "Pier and abutment scour: Integrated approach." J. Hydraul. Eng.-ASCE, 123(2), 125-136.

Melville, B. W., and Chiew, Y. M. (1999). "Time scale for local scour at bridge piers." J. Hydraul. Eng.-ASCE, 125(1), 59-65.

Melville, B. W., and Coleman, N. L. (2000). Bridge Scour, Water Resources Publications, LLC, Highlands Ranch, CO.

Melville, B. W., and Raudkivi, A. J. (1996). "Effects of foundation geometry on bridge pier scour." Journal of Hydraulic Engineering, American Society of Civil Engineers, 122(4), 203–209.

Melville, B. W., and Sutherland, A. J. (1988). "Design method for local scour at bridge piers." Journal of Hydraulic Engineering, 114(10).

Mia, F., and Nago, H. (2003). "Design method of time-dependent local scour at circular bridge pier." J. Hydraul. Eng.-ASCE, 129(6), 420-427.

Mia, M. F., and Nago, H. (2004). "Closure to "Design method of time-dependent local scour at circular bridge pier" by Md. Faruque Mia and Hiroshi Nago." J. Hydraul. Eng.-ASCE, 130(12), 1213-1213.

Miller, W., and Sheppard, D. M. (2002). "Time Rate of Local Scour at a Circular Pile." In: First International Conference on Scour Of Foundations, College Station, Texas, USA, 827-841.

Moreno, M., Birjukova, O., Grimaldi, C., Gaudio, R., and Cardoso, A. H. (2017). "Experimental study on local scouring at pile-supported piers." Acta Geophysica, 65(3), 411–421.

Moreno, M., Maia, R., and Couto, L. (2016). "Prediction of Equilibrium Local Scour Depth at Complex Bridge Piers." Journal of Hydraulic Engineering, 142(11), 04016045.

Moreno, M., Muralha, A., Couto, L., Maia, R., and Cardoso, A. H. (2015). "Influence of column width on the equilibrium scour depth at a complex pier." Proceedings of 36th IAHR World Congress, the Hague, The Netherlands, 1–8.

Mueller, D. S., and Wagner, C. R. (2005). "Field Observations and Evaluations of Streambed Scour at Bridges." Office of Engineering Research and Development Federal Highway Administration, McLean, VA.

Mueller, D. S., and Wagner, C. R. (2002). "Analysis of Pier Scour Predictions and Real-Time Field Measurements." First International Conference on Scour of Foundations, College Station, TX.

National Academies of Sciences, Engineering, and Medicine (2004). Methodology for Predicting Channel Migration. Washington, DC: The National Academies Press. https://doi.org/10.17226/23352.

National Academies of Sciences, Engineering, and Medicine (2011). Scour at Wide Piers and Long Skewed Piers. Washington, DC: The National Academies Press. https://doi.org/10.17226/14426.

Neill, C. R. (1964). "River bed scour, a review for bridge engineers." Research Council of Alberta, Calgary, Alberta, Canada.

Neill, C. R. (1973). "Guide to bridge hydraulics." Roads and Transportation Assoc. of Canada, University of Toronto Press, Toronto, Canada, 191pp.

Neill, C. R., and Robert, C. (1964). "River-bed scour: a review for bridge engineers." Canadian Good Roads, Association.

Nicollet, G., and Ramette, M. (1971). "Affouillements au voisinage de piles de pont cylindriques circulaires." In: Proc. 14th IAHR Congress, Paris, pp. 315-322.

Noormets, R., Ernstsen, V. B., Bartholoma, A., Flemming, B. W., and Hebbeln, D. (2006). "Implications of bedform dimensions for the prediction of local scour in tidal inlets: a case study from the southern North Sea." Geo-Mar. Lett., 26(3), 165-176.

Oliveto, G. (2012). "Temporal variation of local scour at bridge piers with complex geometries." 6th Int. Conf. On Scour Erosion ISCE-6, 167–173.

Oliveto, G., and Hager, W. H. (2002). "Temporal evolution of clear-water pier and abutment scour." J. Hydraul. Eng.-ASCE, 128(9), 811-820.

Oliveto, G., and Hager, W. H. (2005). "Further results to time-dependent local scour at bridge elements." J. Hydraul. Eng.-ASCE, 131(2), 97-105.

Oliveto, G., and Hager, W. H. (2006). "Closure of "Further results to time-dependent local scour at bridge elements" by Giuseppe Oliveto and Willi H. Hager." J. Hydraul. Eng.-ASCE, 132(9), 997-998.

Oliveto, G., Di Domenico, A., and Comuniello, V. (Year). "Temporal development of live-bed scour at bridge piers." Proc. 32nd Congress AHR, Venice, Italy.

Oliveto, G., Onorati, B., and Comuniello, V. (2006). "Effects of pile caps on local scour at bridge piers." Proceedings 3rd International Conference on Scour and Erosion (ICSE-3). November 1-3, 2006, Amsterdam, The Netherlands, 508–512.

Oliveto, G., Rossi, A., and Hager, W. H. (2004). "Time-Dependent Local Scour at Piled Bridge Foundations, Hydraulics of Dams and River Structures." Proceedings of the International Conference on Hydraulics of Dams and River Structures.

Oliveto, G., Unger, J., and Hager, W. H. (2004). "Discussion of "Design method of time-dependent local scour at circular bridge pier" by Md. Faruque Mia and Hiroshi Nago." J. Hydraul. Eng.-ASCE, 130(12), 1211-1213.

Parola, A. C., Mahavadi, S. K., Brown, B. M., and El Khoury, A. (1996). "Effects of rectangular foundation geometry on local pier scour." Journal of Hydraulic Engineering, American Society of Civil Engineers, 122(1), 35–40.

Pilarczyk, K. W. (1995). "Design tools related to revetments including riprap." In: River, Coastal and Shoreline Protection. Erosion Control Using Riprap and Armourstone, John Wiley & Sons, New York, 17-38.

Raikar, R. V., and Dey, S. (2005). "Clear-water scour at bridge piers in fine and medium gravel beds." Can. J. Civ. Eng., 32(4), 775-781.

Raikar, R. V., and Dey, S. (2005). "Scour of gravel beds at bridge piers and abutments." Proc. Inst. Civil. Eng.-Water Manag., 158(4), 157-162.

Raikar, R. V., and Dey, S. (2006). "Pier scour and thin layered bed scour within a long contraction." Can. J. Civ. Eng., 33(2), 140-150.

Raju, K. G. R., and Soni, J. P. (1976). "Geometry of Ripples and Dunes in Alluvial Channels." Journal of Hydraulic Research, 14(3).

Ramos, P. X., Bento, A. M., Maia, R., and Pêgo, J. P. (2016). "Characterization of the scour cavity evolution around a complex bridge pier." Journal of Applied Water Engineering and Research, Taylor & Francis, 4(2), 128–137.

Raudkivi, A. J., and Ettema, R. (1977). "Effect of sediment gradation on clear water scour." Journal of the Hydraulics Division, 103(10), 1209-1213.

Richardson, E. V., and Davis, S. R. (1995). "Evaluating scour at bridges." FHWA-IP-90-017, Third Edition, Office of Technology Applications, HTA-22, Federal Highway Administration, U.S. Department of Transportation, Washington, D.C., U.S.A.

Richardson, J. R., and Trivino, R. (2002). "Clear-water abutment scour prediction for simple and complex channels." In: Hydrology, Hydraulics, and Water Quality; Roadside Safety Features 2002, Transportation Research Board Natl Research Council, Washington, 23-30.

Roulund, A., Sumer, B. M., Fredsoe, J., and Michelsen, J. (2005). "Numerical and experimental investigation of flow and scour around a circular pile." J. Fluid Mech., 534, 351-401.

Rudolph, D., K.J. Bos, Luijendijk, A. P., Rietema, K., and Out, J. M. M. (Year). "Scour around offshore structures -analysis of field measurements." Second Int. Conference on Scour and Erosion, Singapore.

Scacchi, G., Schreider, M., and Fuentes, R. (2005). "Abutment scour at the relief bridge placed in a flood plain." Ing. Hidraul. Mex., 20(3), 43-59.

Shelden, J. G., Pe, M., Smith, E. D., Ei, M., Sheppard, D. M., and Mufeed Odeh, P. E. (Year). "Hydraulic Modeling and Scour Analysis for the San Francisco-Oakland Bay Bridge."

Shen, H. W. (1971). "Scour near piers." Colorado State University, Fort Collins, CO.

Shen, H. W., Schneider, V. R., and Karaki, S. S. (1966). "Mechanics of Local Scour." U.S. Department of Commerce, National Bureau of Standards, Institute for Applied Technology, Fort Collins, Colorado.

Shen, H. W., Schneider, V. R., and Karaki, S. S. (1969). "Local scour around bridge piers." Journal of the Hydraulics Division, 95(HY6), 1919-1940.

Sheppard, D. M. (1997). "Conditions of maximum local scour." University of Florida, Coastal and Oceanographic Engineering Dept., Gainesville, FL.

Sheppard, D. M. (2004). "Overlooked local sediment scour mechanism." In: Highway Facility Design 2004; Including 2004 Thomas B. Deen Distinguished Lecture, Transportation Research Board Natl Research Council, Washington, 107-111.

Sheppard, D. M. (2004). "Overlooked local sediment scour mechanism." Transportation Research Record: Journal of the Transportation Research Board, 1890, 107-111.

Sheppard, D. M. (2005). FDOT Bridge Scour Manual. STATE OF FLORIDA DEPARTMENT OF TRANSPORTATION, Tallahassee, Florida.

Sheppard, D. M. (Year). "A Method for Scaling Local Sediment Scour Depths from Model to Prototype." Joint Conference on Water Resources Engineering and Water Resources Planning and Management Conference, Minneapolis, MN.

Sheppard, D. M. (Year). "Physical Model Local Scour Studies of the Woodrow Wilson Bridge Piers." Joint Conference on Water Resources Engineering and Water Resources Planning and Management Conference, Minneapolis, MN.

Sheppard, D. M., and Jones, J. S. (1998). "Scour at Complex Pier Geometries." Compendium of Scour Papers from ASCE Water Resources Conferences.

Sheppard, D. M., and Jones, J. S. (1998). "Scour at complex pier geometries." In: Compendium of scour papers from ASCE Water Resources Conferences, E. V. Richardson and P. F. Lagasse, eds., ASCE, New York.

Sheppard, D. M., and Jones, S. (Year). "Local Scour at Complex Piers." Joint Conference on Water Resources Engineering and Water Resources Planning and Management Conference, Minneapolis, MN.

Sheppard, D.M., Demir, H., and Melville, B. (2011). "Scour at Wide Piers and Long Skewed Piers." NCHRP Rep. 682, Transportation Research Board, National Academies, Washington, DC.

Sheppard, D.M., Melville, B., and Demir, H. (2014). "Evaluation of Existing Equations for Local Scour at Bridge Piers." J. Hydraul. Eng-ASCE., 140(1), 14-23.

Sheppard, D. M., and Miller, W. (2006). "Live-bed local pier scour experiments." J. Hydraul. Eng.-ASCE, 132(7), 635-642.

Sheppard, D. M., and Ontowirjo, B. (1994). "A local sediment scour prediction equation for circular piles." University of Florida, Coastal and Oceanographic Engineering Dept., Gainesville, FL.

Sheppard, D. M., Odeh, M., and Glasser, T. (2002). "Large scale clear-water local pier scour experiments." Civil & Coastal Engineering Dept., University of Florida, Gainesville, FL.

Sheppard, D. M., Odeh, M., and Glasser, T. (2004). "Large scale clear-water local pier scour experiments." J. Hydraul. Eng.-ASCE, 130(10), 957-963.

Sheppard, D. M., Odeh, M., Glasser, T., and Pritsivelis, A. (2000). "Clearwater Local Scour Experiments with Large Circular Piles." In: Joint Conference on Water Resources Engineering and Water Resources Planning and Management Conference, Minneapolis, MN.

Sheppard, D. M., Odeh, M., Pritsvelis, A., and Glasser, T. (Year). "Clearwater Local Scour Experiments in a Large Flume." Joint Conference on Water Resources Engineering and Water Resources Planning and Management Conference, Minneapolis, MN.

Sheppard, D. M., Sheldon, J., Smith, E., and Odeh, M. (Year). "Hydraulic Modeling and Scour Analysis for the San Francisco-Oakland Bay Bridge." Joint Conference on Water Resources Engineering and Water Resources Planning and Management Conference, Minneapolis, MN.

Sheppard, D. M., Zhao, G., and Ontowirjo, B. (1999). "Local scour near single piles in steady currents." In: Stream Stability and Scour at Highway Bridges, Compendium of Papers, ASCE Water Resources Engineering Conferences 1991-1998, E. V. Richardson and P. F. Lagasse, eds., 1809-1813.

Shields, A. (1936). "Anwendung der Aehnlichkeitsmechanik und der turbulenz forschung auf die geschiebebewegung." Mitt. Preuss. Vesuchanstalt Wesserbau Schiffbau, Berlin, Germany.

Shinohara, K., and Tsubaki, T. (1959). "On the characteristics of sand waves formed upon the beds of the open channels and rivers."

Simarro-Grande, G., and Martin-Vide, J. P. (2006). "Local scour in a protruding wall on a river bank." Ing. Hidraul. Mex., 21(1), 17-27.

Sleath, J. F. A. (1984). Sea bed mechanics, John Wiley & Sons New York, New York.

Snamenskaya, N. S. (1969). "Morphological principle of modelling river-bed process." Science Council of Japan, Tokyo, Japan, 5-1.

Sousa, A. M., and Ribeiro, T. P. (2019). "Local scour at complex bridge piers – experimental validation of current prediction methods." ISH Journal of Hydraulic Engineering, 1–8.

Sturm, T. W. (2006). "Scour around bankline and setback abutments in compound channels." J. Hydraul. Eng.-ASCE, 132(1), 21-32.

Sui, J. Y., Fang, D. X., and Karney, B. W. (2006). "An experimental study into local scour in a channel caused by a 90 degrees bend." Can. J. Civ. Eng., 33(7), 902-911.

Sumer, B. M., and Fredsoe, J. (2002). The Mechanics of Scour in the Marine Environment, World Scientific, Singapore.

Talebi, S., Minor, H. E., and Ortmanns, C. (2004). "Evaluating the time effect on scour and comparing the different experimental and semi-experimental formulas." In: Second Int. Conference on Scour and Erosion, Singapore.

Tison, L. J. (Year). "Erosion autour de piles de ponts en riviere." 813-817.

U.S. Army Corps of Engineers (2002). Coastal Engineering Manual. USACE Engineer Manual 1110-2-1100. Washington, DC, 6 volumes.

Umeda, S., Yamazaki, T., and Yuhi, M. (2010). "An experimental study of scour process and sediment transport around a bridge pier with foundation." Scour and Erosion, 66–75.

Unger, J. (2006). "The flow characteristics around a circular cylindrical pier - Strömungscharakteristika um kreiszylindrische Brückenpfeiler," Ph.D thesis (197), ETH Zürich, Zürich, Switzerland (in German).

Unger, J., and Hager, W. H. (2006). "Riprap failure at circular bridge piers." J. Hydraul. Eng.-ASCE, 132(4).

Van Rijn, L. C. (1993). Principles of sediment transport in rivers, estuaries and coastal seas, Aqua publications, Amsterdam, The Netherlands.

Veerappadevaru, G., Gangadharaiah, T., and Jagadeesh, T. R. (2011). "Vortex scouring process around bridge pier with a caisson." Journal of hydraulic research, Taylor & Francis, 49(3), 378–383.

Venkatadri, C. (1965). "Scour around bridge piers and abutments." In: Irrigation Power, 35-42.

Whitbread, J. E., Benn, J. R., and Hailes, J. M. (2000). "Cost-effective management of scour-prone bridges." Proc. Inst. Civil Eng.-Transp., 141(2), 79-86.

White, W. R. (Year). "Scour around bridge piers in steep streams." 16th IAHR Congress, Sao Paulo, Brazil, 279–284.

Whitehouse, R. (2004). "Marine scour at large foundations." In: Second Int. Conference on Scour and Erosion, Singapore, 455-463.

Yang, Y., Melville, B. W., Sheppard, D. M., and Shamseldin, A. Y. (2018). "Clear-water local scour at skewed complex bridge piers." J. Hydraul. Eng, 144(6), 04018019.

Yang, Y., Melville, B. W., Sheppard, D. M., and Shamseldin, A. Y. (2019). "Live-bed scour at wide and long-skewed bridge piers in comparatively shallow water." Journal of Hydraulic Engineering, American Society of Civil Engineers, 145(5), 06019005.

Yanmaz, A. M. (2006). "Temporal variation of clear water scour at cylindrical bridge piers." Can. J. Civ. Eng., 33(8), 1098-1102.

Yanmaz, A. M., and Cicekdag, O. (2001). "Composite reliability model for local scour around cylindrical bridge piers." Can. J. Civ. Eng., 28(3), 520-535.

Zarrati, A. R., Nazariha, M., and Mashahir, M. B. (2006). "Reduction of local scour in the vicinity of bridge pier groups using collars and riprap." J. Hydraul. Eng.-ASCE, 132(2), 154-162.